

DOKUZ EYLÜL UNIVERSITY
GRADUATE SCHOOL OF NATURAL AND APPLIED
SCIENCES

EFFECT OF SPIRAL ANGLE ON STRESS
DISTRIBUTION IN THE SPIRAL BEVEL GEARS

by
Bengi ÖZBAĞCI

March, 2012
İZMİR

EFFECT OF SPIRAL ANGLE ON STRESS DISTRIBUTION IN THE SPIRAL BEVEL GEARS


**A Thesis Submitted to the
Graduate School of Natural and Applied Sciences of Dokuz Eylül University
In Partial Fulfillment of the Requirements for the Degree of Master of Science
in Mechanical Engineering, Mechanics Program**

**by
Bengi ÖZBAĞCI**

**March, 2012
İZMİR**

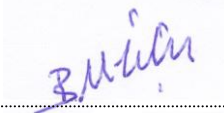
M.Sc THESIS EXAMINATION RESULT FORM

We have read the thesis entitled “EFFECT OF SPIRAL ANGLE ON STRESS DISTRIBUTION IN THE SPIRAL BEVEL GEARS” completed by **BENGİ ÖZBAĞCI** under supervision of **ASSOCIATE PROFESSOR BİNNUR GÖREN KIRAL** and we certify that in our opinion it is fully adequate, in scope and in quality, as a thesis for the degree of Master of Science.




Assoc. Prof. Binnur GÖREN KIRAL

Supervisor



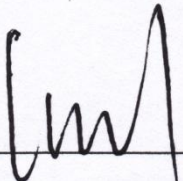
Assoc. Prof. Bülent Murat İÇTEN

(Jury Member)



Assoc. Prof. Mustafa TOPARLI

(Jury Member)



Prof.Dr. Mustafa SABUNCU

Director

Graduate School of Natural and Applied Sciences

ACKNOWLEDGEMENTS

I would like to thank my supervisor, Assoc. Prof. Dr. Binnur GÖREN KIRAL for her patience, excellent guidance, invaluable support and continuous encouragement throughout this study.

I would also like to thank Assoc. Prof. Dr. Zeki KIRAL for his help and suggestions to my master thesis.

I would also like to thank İzmir Metropolitan Municipality General Directorate of ESHOT for their technical supports.

I would also like to thank my friend Mustafa TABANOĞLU for supporting.

Finally, this work is dedicated to my daughter Özgün ÖZBAĞCI, my wife Özlem ÖZBAĞCI and my parents. Their love, continuous and unconditional support inspired me.

Bengi ÖZBAĞCI

EFFECT OF SPIRAL ANGLE ON STRESS DISTRIBUTION IN THE SPIRAL BEVEL GEARS

ABSTRACT

Gear systems are widely used to transmit power or rotary motion in high efficiency. Bevel gear systems are gears which their shafts are not parallel to each other and provide to transmit the torque and power at a desired angle. The main application of the spiral bevel gear system is in a vehicle differential.

Spiral angle of the spiral bevel gear affects the stress distribution on the gear system significantly as well as vibration and noise. In this study, effect of the spiral angle on the stress and deformation that occur in teeth of different types of spiral bevel gear systems are investigated using the finite element method.

First, four different gear systems are modeled in order to determine the effect of the spiral angle on the variation of the stress distribution. Then, three-dimensional contact analyses are performed by ANSYS Workbench commercial software.

Stress, strain and displacement distributions occurred in the spiral bevel gears systems are examined and it is seen that the results obtained in this study are compatible with the results in the literature.

Keywords: Spiral bevel gears, spiral angle, finite element method.

SPİRAL KONİK DİŞLİLERDEKİ GERİLME DAĞILIMINA SPİRAL AÇISININ ETKİSİ

ÖZ

Dışlı çark sistemleri, yüksek verimlilikle güç ya da dönme hareketini iletmek için yaygın olarak kullanılmaktadır. Konik dişli çark sistemleri, mil eksenleri birbirine paralel olmayan ve istenilen bir açı ile moment ve güç iletilmesini sağlayan dişlilerdir. Spiral konik dişli sisteminin ana uygulaması araç diferansiyelindedir.

Spiral konik dişlinin spiral açısı, titreşim ve sesin yanı sıra dişli sistemi üzerindeki gerilme dağılımını da oldukça etkilemektedir. Bu çalışmada, spiral açısının farklı tipteki spiral konik dişli çarkların dişlerinde oluşan gerilme ve deformasyonların üzerine etkisi sonlu elemanlar yöntemi kullanılarak incelenmektedir.

Öncelikle, gerilme dağılımının değişimi üzerine spiral açısının etkisini belirlemek için dört farklı dişli sistemi modellenmiştir. Ardından, ANSYS Workbench ticari yazılımı ile üç boyutlu temas analizleri gerçekleştirilmiştir.

Spiral konik dişli sistemlerinde meydana gelen gerilme, zorlanma ve yer değiştirme dağılımları incelenmiş ve bu çalışmada elde edilen sonuçların literatürdeki sonuçlarla uyumlu olduğu görülmüştür.

Anahtar kelimeler: Spiral konik dişliler, spiral açısı, sonlu elemanlar yöntemi.

CONTENTS

	Page
M.Sc THESIS EXAMINATION RESULT FORM.....	ii
ACKNOWLEDGEMENTS	iii
ABSTRACT.....	iv
ÖZ	v
 CHAPTER ONE - INTRODUCTION	 1
 1.1 Literature	 2
1.2 Purpose of The Thesis	6
 CHAPTER TWO - SPIRAL BEVEL GEAR	 8
 2.1 Bevel Gears	 8
2.2 Load-Carrying Capability.....	13
2.3 Spiral Bevel Gear	14
 CHAPTER THREE - DESIGN, MODELLING AND MATERIAL SELECTION	 17
 3.1 Design, Modelling and Material Selection.....	 18
3.1.1 Loading	18
3.1.2 Material Selection	19
3.1.3 Design	21
3.1.4 Modeling.....	26
 CHAPTER FOUR - FINITE ELEMENT ANALYSIS	 29
 4.1 Finite Element Method	 29

4.2	Analysis Phases	33
4.3	Analysis Results	35
4.3.1	Strains	35
4.3.1.1	Equivalent (von-Mises) Elastic Strain.....	36
4.3.1.2	Maximum Principal Elastic Strain	38
4.3.1.3	Maximum Shear Elastic Strain.....	39
4.3.1.4	Normal Elastic Strain	41
4.3.2	Stresses.....	43
4.3.2.1	Equivalent Stress	43
4.3.2.2	Maximum Principal Stress	45
4.3.2.3	Maximum Shear Stress.....	46
4.3.2.4	Normal Stress	48
4.3.3	Deformation Comparison	50
4.3.3.1	Total Deformation	50
4.3.3.2	Directional Deformation.....	53
4.3.4	Contact Surface Status	55
4.3.5	Safety Factor	56
CHAPTER FIVE - CONCLUSIONS.....		63
REFERENCES.....		65

CHAPTER ONE

INTRODUCTION

A gear is a mechanical device often used in transmission systems that allow rotational force to be transferred to another gear or device. The gear teeth, or cogs, allow force to be fully transmitted without slippage and depending on their configuration, can transmit forces at different speeds, torques, and even in a different direction. Throughout the mechanical industry, many types of gears exist with each type of gear possessing specific benefits for its intended applications (Brown, 2009).

Gears are machine elements that transmit motion by means of successfully engaging teeth. Of two gears that run together, the one with the larger number of teeth is called the “gear.” The “pinion” is the gear with the smaller number of teeth. A rack is a gear with teeth spaced along a straight line and is suitable for straight-line motion. Many kinds of gears are in general use. For each application, the selection will vary depending on the factors involved. One basic rule of gearing is that to transmit the same power, more torque is required as speed is reduced. The torque is directly proportional to speed, and therefore, the input and output torques for power transmission are directly proportional to the ratio if efficiency is neglected. Gearing gives the engineer the flexibility to make the machine system fit the job, not the other way around. The power loss of 1.25 to 4.0 percent is a small price to pay for the advantages obtained (Bloch & Geitner, 1996).

Gears are usually used to change the speed of the driven equipment from that of the driver, to alter the direction of power flow, or to change rotation direction. In very few cases are the most efficient design speeds of a driver and driven machine identical. Probably the most common example we see of this is the modern automobile where we use gearing to change both the speed and the direction of power flow from the engine to the wheels. In this case, the reciprocating engine would be extremely large should gearing not be available to change the speed (Bloch & Geitner, 1996).

1.1 Literature

Lin, Ou and Li presented an approach for mesh generation of gear drives at any meshing position and developed an automatic modeling program for tooth mesh analysis. Based on the derivation of a flexibility matrix equation in the contact region, a finite element method for 3D contact/impact problem was proposed. Using this method, tooth load distribution and mesh stiffness results were derived under static loading during meshing process. This method was also used to simulate the gear behavior under dynamic loading conditions. The dynamic responses of the gear drives were obtained under the conditions of both the initial speed and the sudden load being applied. In their studies, the influence of the backlash on impact characteristics of the meshing teeth was analyzed (Lin, Ou & Li, 2006).

Simon presented a new method for computer aided tooth contact analysis in mismatched spiral bevel gears. As the introduced tooth surface modifications in spiral bevel gears were relatively small and the conjugation of the mating surfaces is relatively good, thus it was assumed that the theoretical point contact of mismatched spiral bevel gears under load spreads over a surface along the whole or part of the “potential” contact line made up of the points of the meshing teeth surfaces in which the geometrical separations of these surfaces along the tooth face width are minimal. The method was based on the minimization of the function that determines these separations, defined as the distances of the corresponding surface points that were the intersection-points of the straight line parallel to the common surface normal in the instantaneous theoretical contact point with the pinion and gear tooth surfaces. The points with these minimal separations made up the potential contact lines. The method included the determination of path of contact and transmission errors, too. By using a computer program developed, the path of contact, the potential contact lines, the separations of the meshing tooth surfaces along these contact lines, the angular displacements of the gear member and the variation of the angular velocity ratio through a mesh cycle were calculated. The influence of machine tool setting and relative position errors of meshing pinion and gear on tooth contact was investigated and discussed (Simon, 2006).

Argyris, Fuentes and Litvin proposed an integrated computerized approach for synthesis, analysis and stress analysis of enhanced spiral bevel gear drives. Their approach was accomplished by application of computerized methods of local synthesis and simulation of meshing and contact of gear tooth surfaces. The developed methods could provide: (i) a localized bearing contact less sensitive to errors of alignment and (ii) reduced vibration and noise. The formation of bearing contact during the cycle of meshing and performing the stress analysis were investigated by performing the finite element analysis. The design of the finite element models and the settings of boundary conditions were automatized. In their study, an integrated computer program for the synthesis, TCA and stress analysis of spiral bevel gear drives was developed. The most time-consuming step in application of finite element analysis, the design of contacting models by using a CAD computer program, is avoided due to automatization of the development of such models. The developed computer programs were based on application of FORTRAN computer language for numerical computations and Visual Fortran QuickWin run-time library for graphical interpretation of results. The proposed approach was applied to the design and stress analysis of face-milled generated spiral bevel gears. Two numerical examples with the output of stress analysis for a finite element model with three pair of teeth were represented. The developed approach may be applied for design of various types of gear drives (Argyris, Fuentes & Litvin, 2002).

Simon, in another study, performed stress analysis in hypoid gears by using finite element method in order to develop simple equations for the calculation of tooth deflections and stresses. Simon applied a displacement type finite element method with curved, twenty-node isoparametric elements. Thus, a method was developed for the automatic finite element discretization of the pinion and the gear. The full theory of mismatched hypoid gears was applied for the determination of the nodal point coordinates on the teeth surfaces. The corresponding computer program is developed. By using this program, the influence of design parameters and load position on tooth deflections and fillet stresses was investigated. He derived on the basis of the results, obtained by performing a big number of computer runs, by using

regression analysis and interpolation functions, equations for the calculation of tooth deflections and fillet stresses (Simon, 2000).

Litvin, Fuentes, Fan and Handschuh proposed a new approach for design, tooth contact analysis and stress analysis of formate generated spiral bevel gears. The advantage of formate generation was the higher productivity. The purposes of the proposed approach were to overcome difficulties of surface conjugation caused by formate generation, develop a low noise and stabilized bearing contact, and perform stress analysis. The approach proposed was based on application of four procedures that enable in sequence to provide a predesigned parabolic function of transmission errors with limited magnitude of maximal transmission errors, a bearing contact with

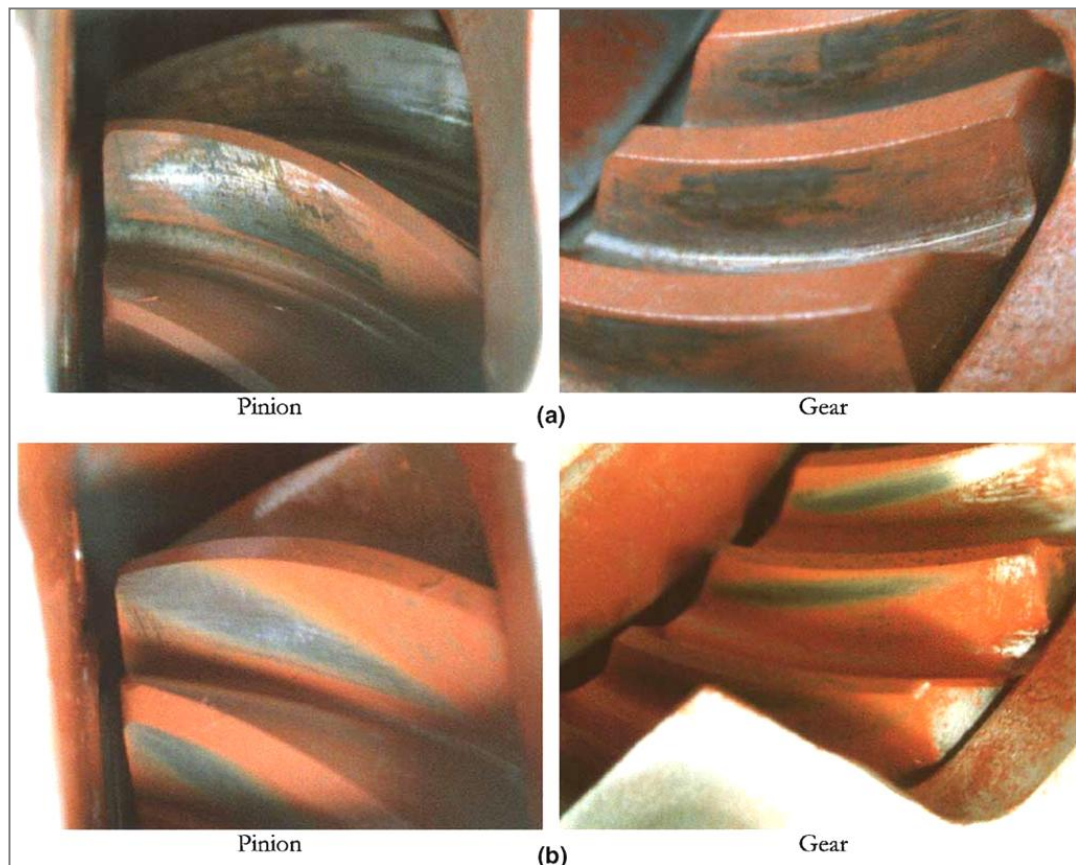


Figure 1.1 Contact patterns on the driving side of gear and driven side of the pinion tooth surfaces without load for (a) existing design and (b) enhanced design based on an adjusted path of contact (Litvin, Fuentes & Hayasaka, 2006).

reduced shift of contact caused by misalignment, and perform stress analysis based on application of the Finite Element Method. The advantage of the approach developed for finite element analysis was the automatic generation of finite element models with multi-pairs of teeth (Litvin, Fuentes, Fan & Handschuh, 2002).

Litvin et al generated an example of enhanced design and optimization of a face-milled spiral bevel gear. The concave side of the pinion tooth surface and the convex side of the gear tooth surface were considered as the driving and driven surfaces, respectively. Figure 1.1 shows the contact patterns of the driving side of gear and pinion tooth surfaces for the unloaded gear drive of previous design (Figure 1.1a), and for the optimized design (Figure 1.1b) based on application of an adjusted path of contact (Litvin, Fuentes & Hayasaka, 2006).

Sheveleva, Volkov, Medvedev represented an algorithm for a geometrical and kinematical analysis of meshing and described two algorithms for a contact stress analysis, which are distinguished from all other known algorithms. The algorithms were based on grid presentation of contacting surfaces and field of distances between them. Also presented are the computer codes for a spiral bevel gear analysis based on these algorithms. The codes provided the contact path, transmission error, bearing contact (assembly of instantaneous contact areas) and contact pressure distribution. The first algorithm for computing of contact pressure used classical Hertz solution; the second one presents non-Hertz solution of contact problem for elastic solids of finite dimensions using boundary element method. The comparison of results provided by these algorithms was presented for a specific spiral bevel gear (Sheveleva, Volkov & Medvedev, 2006).

Most important point of spiral bevel gear manufacturing is right setting of tooth contacts track. If contact doesn't occur on the right area, gears cannot carry the anticipated load and fatigue life will be shorter than expected. Due to these reasons, there are many continuing studies about spiral bevel gears.

1.2 Purpose of The Thesis

In this thesis, stresses and strain distributions on the teeth have been examined with respect to the spiral angle in the spiral bevel gear systems. It is aimed to reduce the stress values by determining the optimum values of spiral angles. Firstly, spiral bevel gear group has been modeled and analyzed by using the computer programs and then, stress and deformation distribution have been examined. Computer-aided design and analysis for spiral bevel gears have been carried out, then distributions of stresses and deformations have been investigated. Sequence for these processes as follows;

1. Parameter Selection and Modeling: Dimensions of the differential gear of the articulated bus are considered for the finite element analyses. Three-dimensional models have been generated in virtual platform by Camnetics GearTeq software and transferred to SOLIDWORKS software. Then, gears which have same teeth number and diameter, but different spiral angle have been modeled by Camnetics GearTeq and then transferred to SOLIDWORKS.

2. Analysis: Three-dimensional models are transferred to Ansys software after the gears are positioned in synchronized by Solidworks. The stress, strain and displacement distribution on the gear in the operation conditions have been obtained by using Ansys Commercial Software with the finite element method.

3. Results: The results obtained by the three-dimensional finite element analyses in this thesis have been compared to that of the studies in the literature. Effects of the spiral angle on the stress, strain and displacement distributions on the modelled gears have been examined.

The studies on the spiral bevel gears are performed by the computer-aided design due to less cost and time consumption. The accurate results can be obtained if the parameters and limit conditions are determined accurately. In this thesis, it is aimed to obtain the optimum spiral angle values for the spiral bevel gears using the finite

element method. Performing the contact analyses, stress and strain distributions on the gear have been determined. Results obtained by carrying out the analyses comprehensively have presented in figures and tables.

CHAPTER TWO

SPIRAL BEVEL GEAR

2.1 Bevel Gears

Bevel gears are useful when the direction of a shaft's rotation needs to be changed. Bevel gears can transfer power between nonparallel shafts. They are usually mounted on shafts that are 90° apart, but can be designed to work at other angles as well.

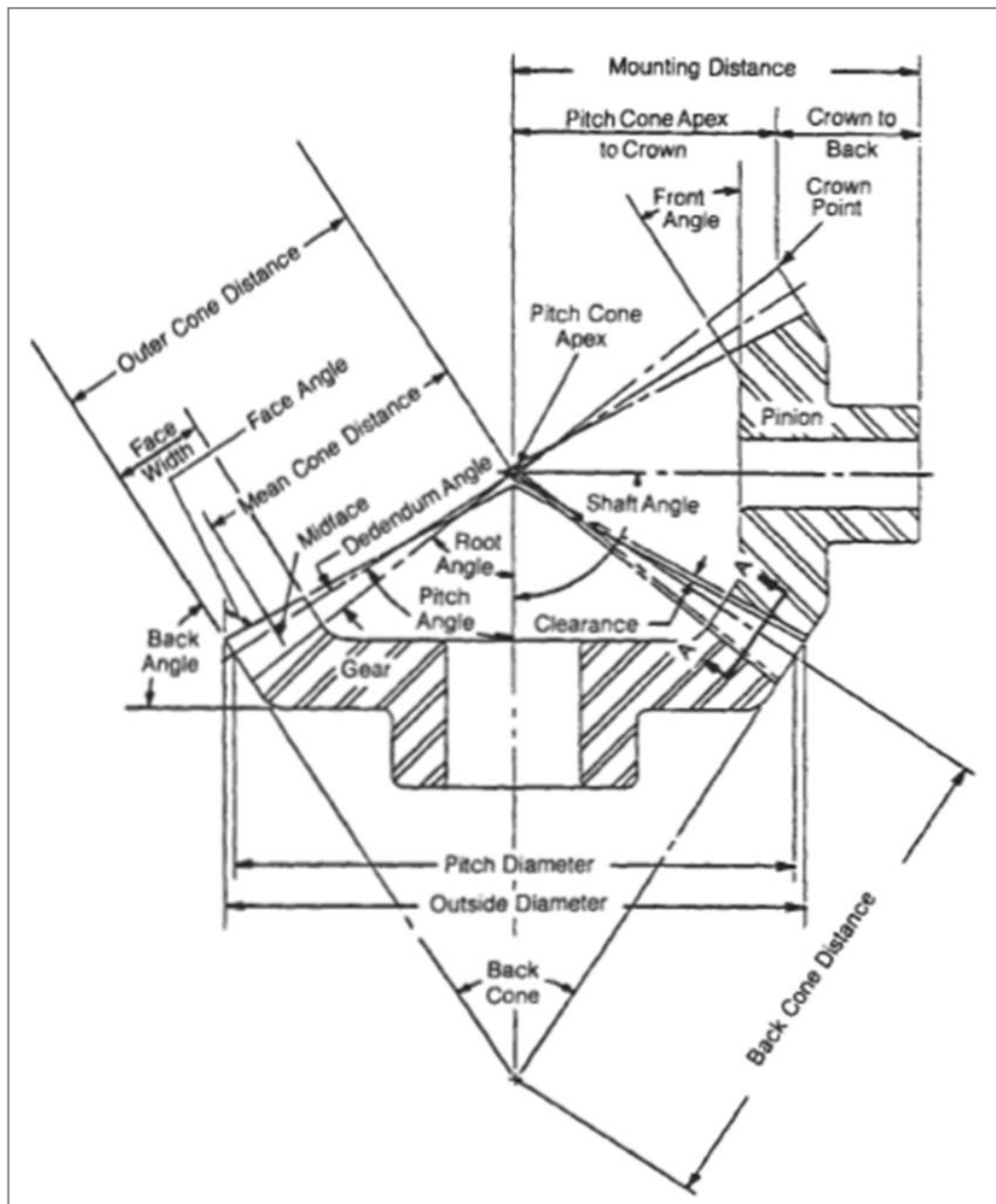


Figure 2.1 Bevel gears geometry (Bloch & Geitner, 1996).

As shown Figure 2.1, the tooth surfaces of bevel gears are conical form. Bevel gears can be defined in four main groups as follows:

1. **Straight Bevel Gear:** The simplest type of bevel gears is straight bevel gears. Straight bevel gears have straight tooth geometry. Teeth extends, passes through the intersection of their axes. (Figure 2.3a)
2. **Spiral Bevel Gear:** Spiral bevel gears have a double function which is helical and beveled. In spiral bevel gears, teeth have spiral angles. Spiral angle allowing tooth contact to be quietly and smooth. Teeth are curved form. Spiral bevel gears suitable for higher speed and higher loaded applications. (Figure 2.3b)
3. **Zerol Bevel Gear:** Zerol bevel gears are the combination of straight and spiral bevel gears. As shown Figure 2.2, actually, zerol bevel gears are spiral bevel gears which spiral angle is zero. (Figure 2.3c)
4. **Hypoid Bevel Gear:** These types of gears are similar to spiral bevel except that the pitch surfaces are hyperboloids rather than cones. Another difference between spiral bevel gears and hypoid bevel gear is hypoid bevel gears axes in different planes. (Figure 2.3d) (Bevel gears, 2011).

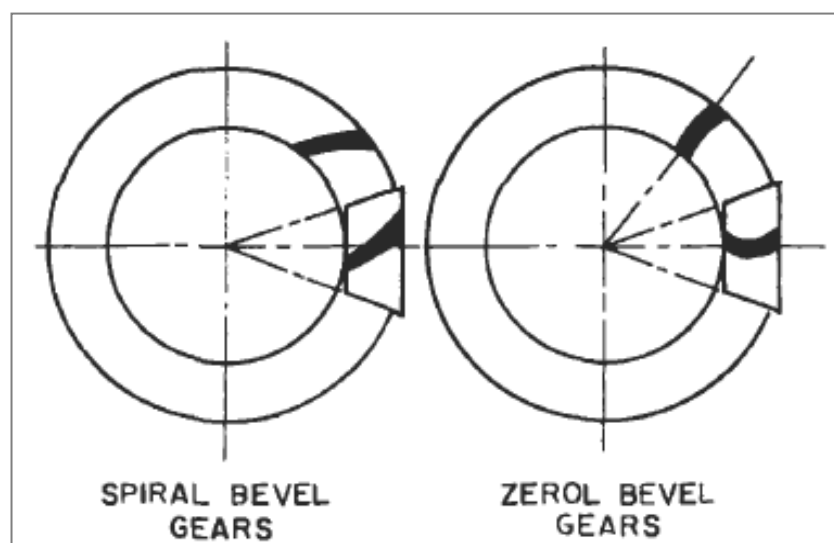


Figure 2.2 Differences between spiral bevel gear and zerol bevel gear (Bloch & Geitner, 1996).

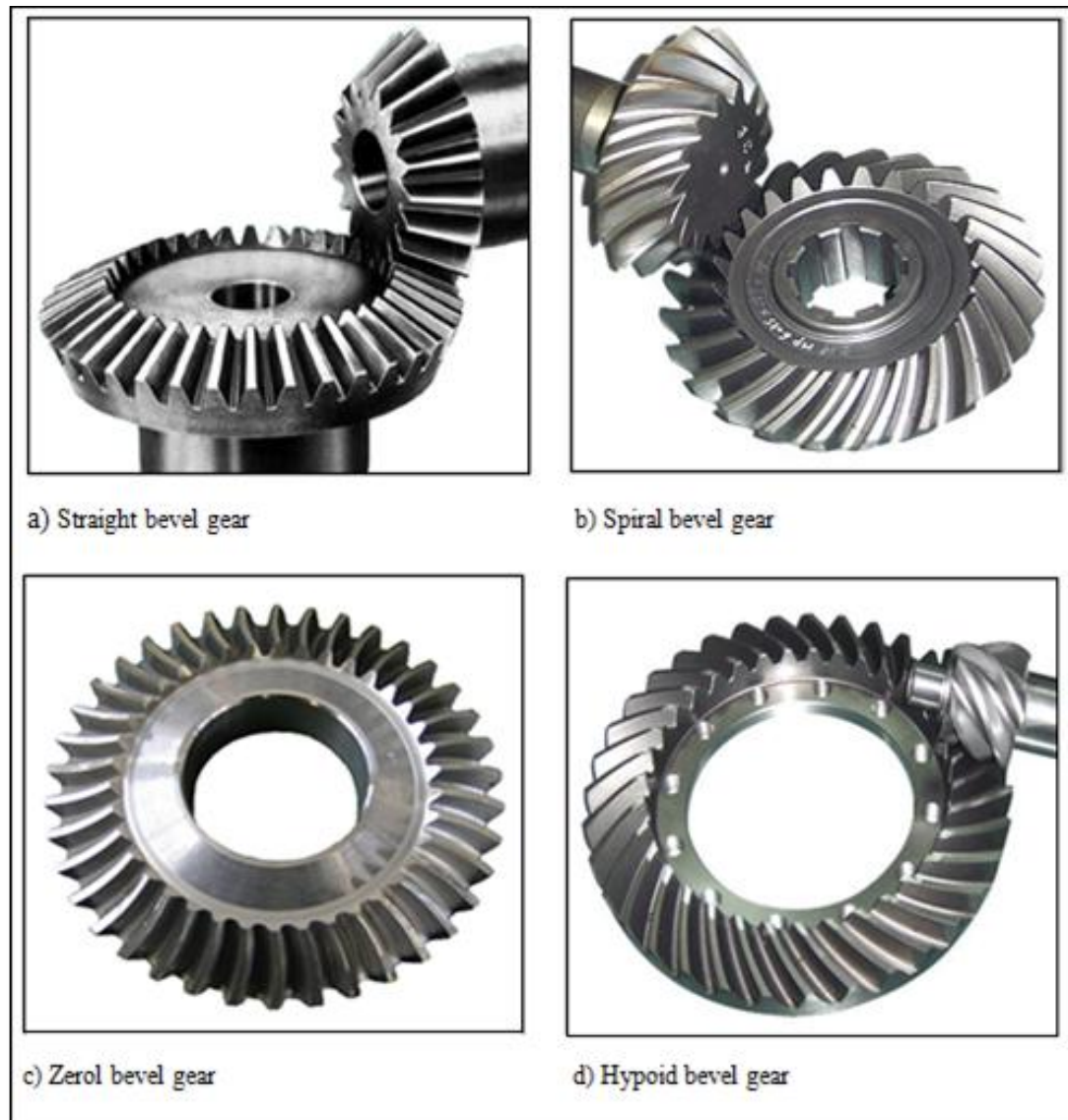


Figure 2.3 Bevel gears types

There are several types of bevel gears according to the axes (Figure 2.4). Most commonly of them are spiral bevel gear, hypoid gear, spiroid gear. Hypoid gears are similar to spiral bevel except that the pitch surfaces are hyperboloids rather than cones. Pinion can be offset above, or below, the gear centre, thus allowing larger pinion diameter, and longer life and smoother mesh, with additional ratios e.g 6:1, 8:1, 10:1. Hypoid gears are best for the applications requiring large speed reductions with non intersecting shafts and those applications requiring smooth and quiet operation. Hypoid gears are generally used for automotive applications. The minimum number of teeth for speed ratios greater than 6 :1 is eight although 6 teeth

pinions can be used for ratios below 6:1. Hypoid gears have pressure angles between 19^0 and 22^0 (Bevel gears, 2011).

Spiroid gears similar to hypoid gears except between axes angle. Spiroid gears between worms gears and hypoid gears. The teeth are curved teeth at an angle allowing tooth contact to be gradual and smooth. These are produced using a spiral gear form which results in a smoother drive suitable for higher speed higher loaded applications. Again satisfactory performance of this type of gear is largely dependent upon the rigidity of the bearings and mountings (Bevel gears, 2011).

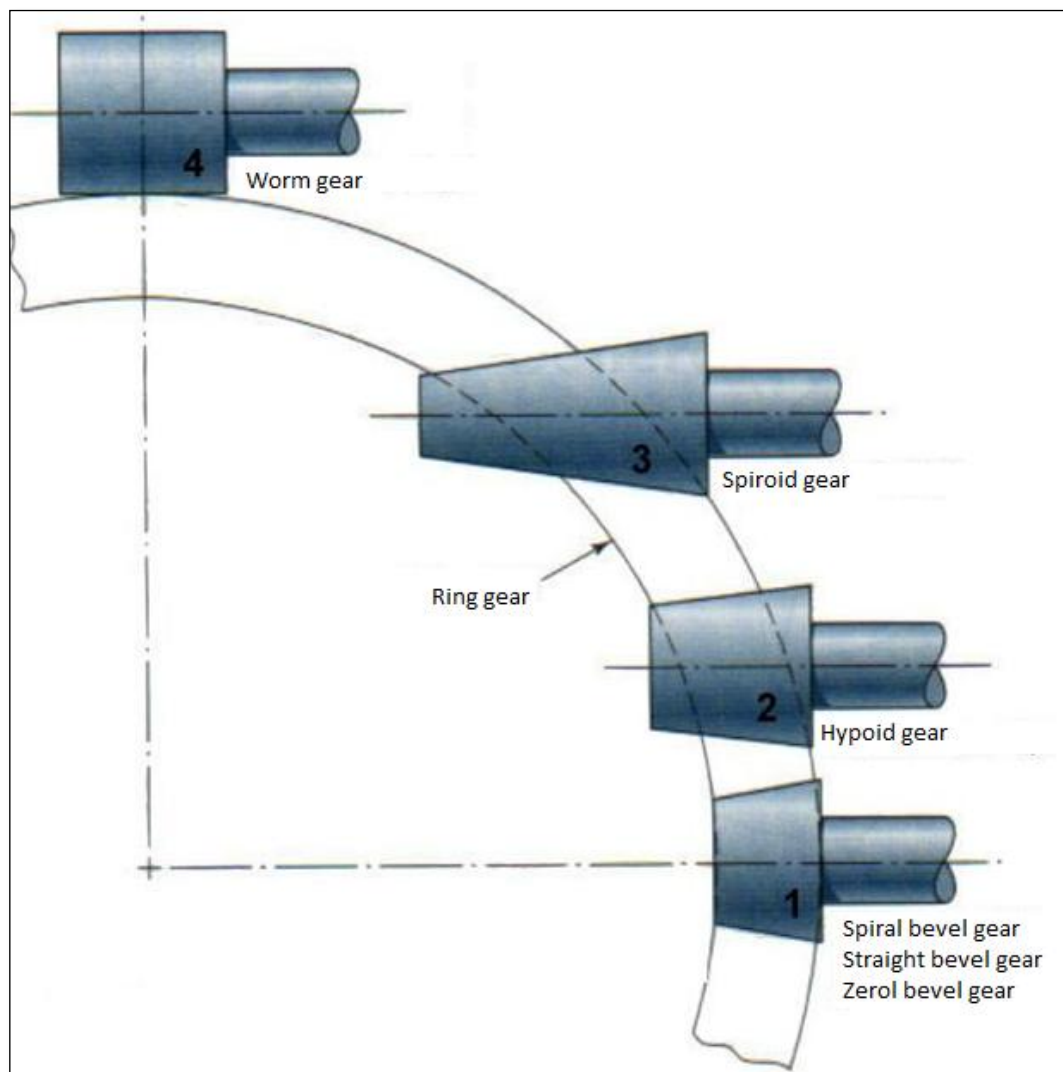


Figure 2.4 Bevel gears according to axes (Shigley, Mischke & Budynas, 2004).

There are three types of bevel gears systems depending on the value of intersection angle (Φ) of shaft axis. ($\Phi < 90^\circ$; $\Phi = 90^\circ$; $\Phi > 90^\circ$). As seen from Figure 2.5, semi-apical angle (δ_p ve δ_w) of cone rolling of bevel gears changes depending on intersection angle of the shaft axes. Value of intersection angle (Φ) ranges between 60° - 120° approximately (Erdirin, 2009).

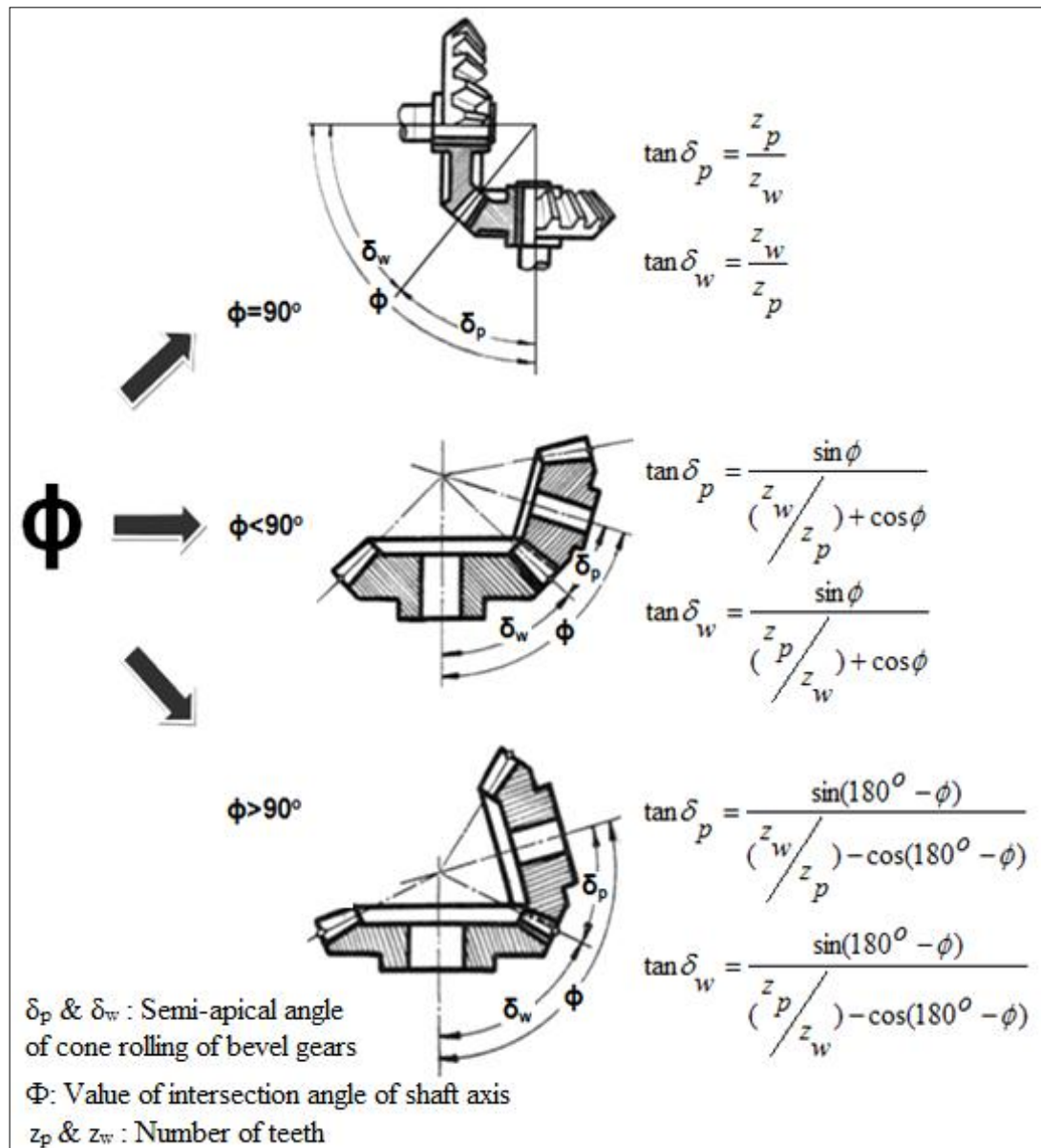


Figure 2.5 Bevel gears with respect to the intersection angle of shaft axes (Doğanay, 1963).

The principles in the straight gears are applied when the tooth force is calculated in the bevel gears calculating.

2.2 Load-Carrying Capability

Plane of the applied force in the bevel gears is assumed as the average plane of gear. Tooth force is,

$$F_n = F_{n1} = F_{n2}$$

Tangential force and radial force are given as ,

$$F_t = F_n \cos \alpha_0 ; F_r^1 = F_t \tan \alpha_0 \quad (\text{Figure 2.6a})$$

In the plane of the real bevel gear , (Figure 2.6b) both radial and tangential forces are

$$F_{r1} = F_{a2} = F_t \tan \alpha_0 \cos \delta_{01} \quad ; \quad F_{a1} = F_{r2} = F_t \tan \alpha_0 \sin \delta_{01}$$

$$F_t = \frac{2M_{bc1}}{d_{0m1}}$$

The stress is computes as follows:

$$\sigma_1 = \frac{F_t}{bm_m} K_{fe1} K_v < \frac{\sigma_{D1}}{S} \quad ; \quad \sigma_2 = \frac{F_t}{bm_m} K_{fe2} K_v < \frac{\sigma_{D2}}{S}$$

K_{fe1} and K_{fe2} are form factor of gears (Table 2.1) (Akkurt, 2000).

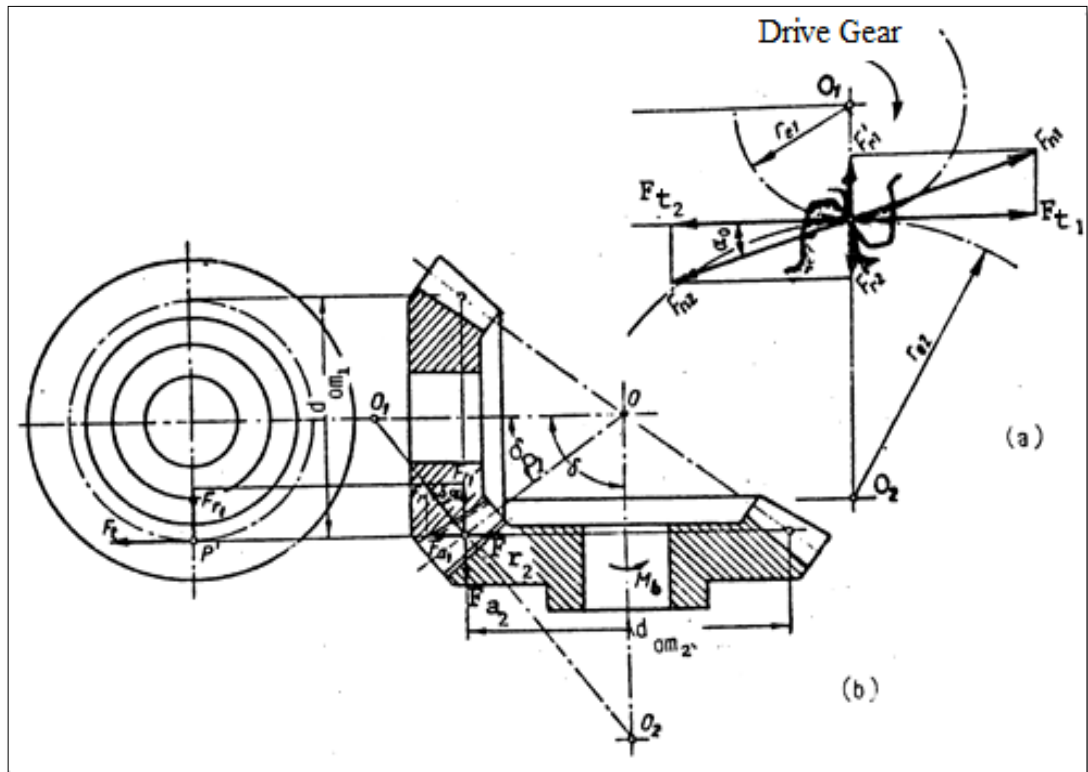


Figure 2.6 Forces in the bevel gears (Akkurt, 2000) .

Table 2.1 Form factor for gears (Akkurt, 2000).

z_e	12	14	15	16	17	18	19	20	21	22	23	24	25	26
K_f	3.7	3.33	3.23	3.15	3.08	3	2.98	2.95	2.9	2.86	2.82	2.78	2.73	2.7
z_e	27	28	29	30	35	40	45	50	65	70	80	90	100	∞
K_f	2.67	2.64	2.62	2.6	2.51	2.45	2.41	2.37	2.29	2.28	2.25	2.23	2.21	2.2

2.3 Spiral Bevel Gear

Spiral bevel gears have curved and sloped gear teeth in relation to the surface of the pitch cone. As a result, an oblique surface is formed during gear mesh which allows contact to begin at one end of the tooth (toe) and smoothly progress to the other end of the tooth (heel). Spiral bevel gears, in comparison to straight or zero bevel gears, have additional overlapping tooth action which creates a smoother gear mesh. This smooth transmission of power along the gear teeth helps to reduce noise and vibration that increases exponentially at higher speeds. Therefore, the ability of a spiral bevel gear to change the direction of the mechanical load, coupled with their ability to aid in noise and vibration reduction, make them a prime candidate for use in the automotive and helicopters industry (Brown, 2009).

High requirements to the reduction of level of noise and the obtaining of favorable shape and dimensions of the bearing contact and the complexity of geometry of gear tooth surfaces complicate the problem of design and geometry of spiral bevel gear drives (Argyris, Fuentes & Litvin, 2002).

The design and generation of spiral bevel gear drives require not only high-quality equipment and tools for manufacturing of such gear drives, but the development of the proper machine-tool settings. Such settings are not standardized, but have to be determined for each case of design (depending on geometric parameters of the gear drive and generating tools) to guarantee the required quality of the gear drives (Litvin, Fuentes & Hayasaka, 2006).

Spiral bevel gears have most complicated design and hardest manufacture

method.(Except specific gear type) . Manufacture of spiral bevel gear needs a serious knowledge and experience. Spiral bevel gears are also known as differential gear. (Aymaksan Dişli, n.d.)

The American Gear Manufacturing Association (AGMA) has developed standards for the design, analysis, and manufacture of bevel gears. The first step in any general design employing gears is to first predict and understand all of the conditions under which the gears will operate. Most importantly are the anticipated loads and speeds which will affect the design of the gear. Additional concerns are the operating environment, lubrication, anticipated life of operation, and assembly processes, just to name a few (Brown, 2009).

According to different manufacturing methods, teeth may be circle arc (GLEASON), evolvent (KLINGELNBERG) or epicycloids (OERLIKON). At the present day, in practice the differences between the gears what are produced with the manufacturing technologies are very small and insignificant for many applications. Because of this, gear geometry is standardized by ISO and ANSI committees. (Aymaksan Dişli, n.d.)

There is no exactly description for spiral bevel gear profiles. Profiles may be different according to manufacturing method and contact track. Pressure angle is usually 20° however; it may change according to contact track and some specific case. Pressure in the contact point spreads over elliptic area. Load in the contact point and curvature of tooth flank generate dimension of elliptic area. Position of gears contact may be controlled through the curvature of tooth (Spiral) . (Aymaksan Dişli, n.d.)

The conditions of meshing and contact of spiral bevel gears depend substantially on the machine-tool settings to be applied. Such settings are not standardized and have to be determined for each case of design depending on the parameters of the gears and generating tools (Argyris et al, 2002).

One of the most important features of spiral bevel gears is their manufacturing as couple. In other words, being same of module and pressure angle is not enough for working together of spiral bevel gear.

The gears discussed are applied in transmissions and reducers for transformation of rotation and torque between intersected axes. The axes of the gears are two cones that roll over each other in the relative motion. The apex angles of the cones are determined as follows:

$$\tan \gamma_1 = \frac{\sin \gamma}{m_{12} + \cos \gamma} \quad , \quad \tan \gamma_2 = \frac{\sin \gamma}{m_{21} + \cos \gamma}$$

where

$$m_{12} = \frac{\omega^{(1)}}{\omega^{(2)}} = \frac{N_2}{N_1} \quad , \quad m_{21} = \frac{1}{m_{12}} = \frac{\omega^{(2)}}{\omega^{(1)}} = \frac{N_1}{N_2}$$

N_1 is number of teeth of pinion, N_2 is number of teeth of gear. $\omega^{(1)}$ is angular velocity of the pinion , $\omega^{(2)}$ is angular velocity of the gear. m_{12} and m_{21} are gear ratio. γ_1 is angles of pinion pitch cones, γ_2 is angles of gear pitch cones (Figure 2.7) (Litvin, Wang & Handschuh, 1997).

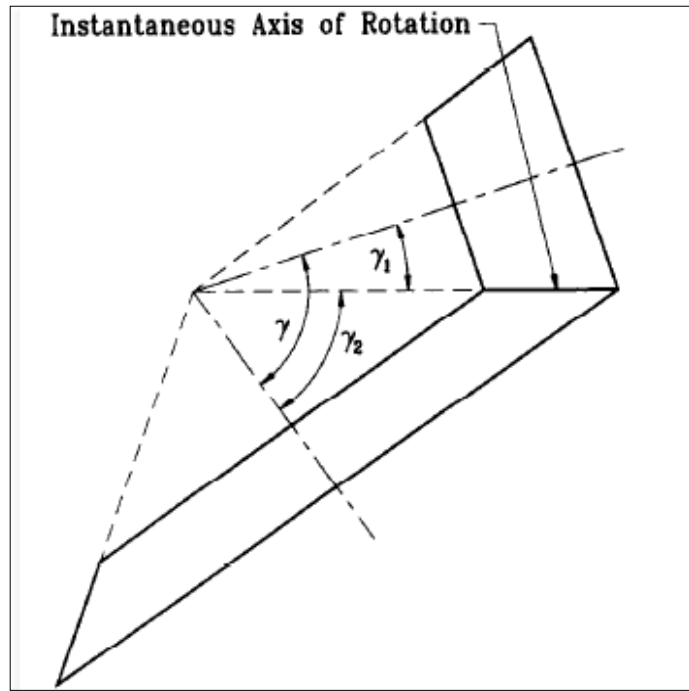


Figure 2.7 Pitch cones (axodes) of bevel gears. (Litvin, Wang & Handschuh, 1997).

CHAPTER THREE

DESIGN, MODELLING AND MATERIAL SELECTION

In this chapter, computer-aided design and solid modeling of spiral bevel gear, and phases of computer-aided analysis by finite elements method will be explained.

In Fig. 3.1, $S(X, Y, Z)$ and $S^1(X^1, Y^1, Z^1)$ are two fixed coordinates connecting to the housing of gear 1 and gear 2. The X -axis and the X^1 -axis are constructed to represent the rotating axes of gear 1 and gear 2, respectively, and the Z -axis and Z^1 -axis coincide with the common normal of the two rotating axes. The notation γ is denoted as the twist angle of the two rotating axes. Assume that ω_1 and ω_2 are the angular velocities of these two gears when the rotating angles are Φ_1 and Φ_2 . The notation m is denoted as the speed ratio of gear 2 to gear 1. In general, most of the speed ratios of gear sets used in industry is constant. According to the screw theory, there must exist a pitch line on the plane constructed by the X -axis and the X^1 -axis, and δ is the angular parameter of the pitch line. According to the screw theory, δ can be described as

$$\delta = \tan^{-1} \left(\frac{m \sin \gamma}{m \cos \gamma - 1} \right)$$

(Tsai & Hsu , 2007).

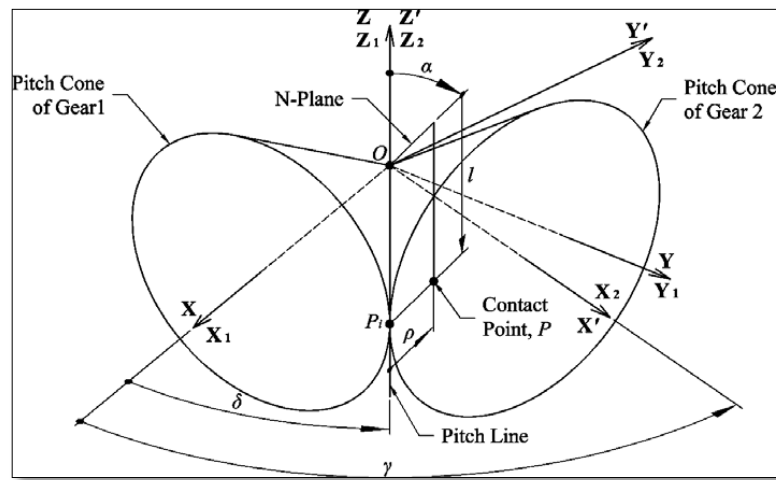


Fig. 3.1 The coordinate system of the bevel gear sets (Tsai & Hsu , 2007).

Spiral bevel gear can transmit high torques and forces to different directions in low sound levels.

3.1 Design, Modelling and Material Selection

The process of designing gear teeth is somewhat arbitrary in that the specific application in which the gear will be used determines many of the key design parameters. Recommended design practices are published in the AGMA standard 2005-D03, Design Manual for Bevel Gear Teeth. This design standard illustrates all aspects of bevel gear tooth design, starting from preliminary design values and progressing towards a finished design ready to be analyzed. Not only does it give recommended practices for design, it also covers manufacturing considerations, inspection methods, lubrication, mounting methods, and appropriate drawing formats. While this is certainly an invaluable tool published in order to provide one guideline for the design of bevel gears across all industries, it does not always properly differentiate design parameters that should be used for one industry versus another. For example, the automotive industry typically uses cast iron gears in transmission applications whereas a cast iron gear would not be feasible in a helicopter transmission because of the high level of loading and occurrence of peak loads that have the potential to be significantly higher than the load at normal operating conditions. As a result, a gear designer must have significant experience in the appropriate industry and be able to make intelligent decisions based on the specific application, which may or may not agree with the AGMA recommendations (Brown, 2009).

3.1.1 Loading

In this study, finite element analyses is performed applying the torque on the spiral bevel gears of differential, using the gearbox and engine data of an articulated bus that is used in local transportation.

Engines repaired at İzmir Metropolitan Municipality General Directorate of ESHOT, are assembled after being tested in the Engine Testing Unit. During the testing process it was observed that the engine produces maximum engine torque between 1350 rpm -1550 rpm. In addition, at the testing unit the maximum engine torque was measured as 98.5 kgm at 1435 rpm, while the maximum torque is 1250 Nm between 1100 rpm -1600 rpm according to the manufacturing data of the engine. It should be taken into account that the engines at the testing unit had been under revision. Therefore, in this thesis the manufacturing data are taken into consideration. The engine manufacturing data are given in Table 3.1. The gear-box used in the vehicle has conversion rate of 5.2 at the first gear, and the conversion rates for the second, third and fourth gears are 1.36, 1 and 0.73, respectively. Thus, the maximum torque delivered to the differential is as follows

$$i = 1250 \times 5,2 = 6500 \text{ Nm}$$

Table 3.1 – Power, torque and engine speed ratings (Daimler-Benz, n.d.).

Max. Torque at 1100-1600 /min	1250 Nm
Minimum engine speed limit under load	1000/min
Maximum permissible engine speed with engine brake operation	2350/min
Minimum idling speed	500/min

3.1.2 Material Selection

The gears designed in this study will be working at high speeds and with heavy loads, considering their places of use. The material is chosen as 14NiCr14. from Table 3.3 because of the operational conditions. The mechanical and physical properties of this material are given in Table 3.2. The carbon percentage of the material is between 0.10%-0.17%. In the manufacturing of these types of gear, carbon amount is high and the surface is hardened by cementation. The material is tempered in the cementation matter between 900 °C - 950 °C and the surface layer that will be hardened is saturated with carbon.

In hardening bevel gears, the applicator coil is wound to conform to the face angle of the gear. In some spiral-bevel gears, there is a tendency to obtain more heat on one side of the tooth than on the other. In some sizes of spiral-bevel gears, this tendency can be overcome by applying slightly more heat to ensure hardening of the concave side. In some forms of spiral-bevel gears, it has been the practice to carburize that part of the gear surface which is to be hardened, after the teeth have been rough-cut. Carburizing is followed by the finish-cutting operation, after which the teeth can be induction heated, using a long enough period to heat the entire tooth. When the gear is quenched, only the carburized surface will become hardened (Oberg, Jones, Horton & Ryffel, 2008).

Table 3.2 Properties of 14NiCr14 (BÖHLER-UDDEHOLM Australia, n.d.).

MECHANICAL PROPERTIES	Diameter	Tensile Strength MPa	Yield Strength MPa	Elong %	Red. Of Area %
	11	980-1280	785	8	35
	30	880-1180	765	9	40
	63	780-1080	635	10	40
PHYSICAL PROPERTIES	Density (kg/m ³)			7850	
	Modulus of elasticity (GPa)			210	

In gear-wheel systems, the gear teeth are subject to repeated loads. In most of the situations, surface pressure values may exceed the material resistance limit. Thence, hardening is important and necessary for gearwheels. The methods used for hardening gearwheels are tempering, normalizing, flame hardening, nitriding and carburization. Gearwheel materials can be separated into eight main groups considering their load capacity and sizes (Table 3.3). Gearwheel materials can be classified in two main groups. A, B, C, D types of material given in Table 3.3 are used to manufacture gearwheels with low surface toughness. In these types of

gearwheels gear teeth are formed after the heat treatment process. E, F, G, H types of materials are used in manufacturing gearwheels with high hardness. In these types of gearwheels, the heat treatment is applied after the gear teeth are formed. Heat treatment processes increase the costs significantly. Also, the complicated finishing processes that are required in order to reach sufficient sensitivity, increase the costs (Erdin, 2009)

3.1.3 Design

Spiral angle and pressure angle are two design parameters that help determine the shape of a spiral bevel gear tooth. Common design practices have determined that for spiral bevel gears, a pressure angle of twenty degrees and a spiral angle of thirty five degrees should be used. Following this common practice for selection of spiral angle establishes a good face contact ratio which maximizes smoothness and quietness during gear mesh. In regards to the selection of a pressure angle, a lower pressure angle increases the transverse contact ratio, a benefit which results in increased bending strength, while also increasing the risk of undercut which is a major concern. Lower pressure angles also help to reduce the axial and separating forces and increase the toplands and slot widths. These factors help to strengthen the gear teeth because the increased slot widths allow the use of larger fillet radii, resulting in increased bending strength. The contact stress is reduced however, as a result of the larger fillet radii, so close consideration is required to ensure the correct pressure angle is chosen for the intended application (Brown, 2009).

Important gear tooth nomenclature;

The following nomenclature is general terms used on the gear drawing. A more complete explanation of terms, definitions and illustrations is given in American Standard for Gear Nomenclature, ANSI/AGMA 112.05, published by the American Gear Manufacturers Association (Whitmire, 2003).

Table 3.3 Gearwheel materials with respect to their load capacity and sizes (Erdin, 2009).

Type	Load	Size	Material
A	Low	Small	Structural Steel St50–2/St52–3/St60–2/St70–2–no process
			Carbon Structural Steel Ck45/Ck60–normalized
			Carbon Structural Steel Ck45/Ck60–heat treatment
B	Low	Large	Nodular DD GGG–60/GGG–70
			Nodular DD GGG–80–heat treatment
			Gray DD GG–20/GG–25/GG–30
C	Medium	Small	Alloy Structural Steel 37Cr4/42CrV6–heat treatment
D	Medium	Large	Nodular DD GGG–60/GGG–70
			Nodular DD GGG–80–heat treatment
			Carbon DD GS–52/GS–60–normalized
			Alloy DD 36Mn5/GS-17CrMoV5 11–normalized
			Alloy DD 36Mn5/GS-17CrMoV5 11–heat treatment
			Alloy Structural Steel 42CrV6/31NiCr14–heat treatment
E	High	Small	Carbon Cast Iron GS–60/36Mn5–gear teeth case-hardened
			Carbon Structural Steel Ck50–gear teeth case-hardened
			Alloy Structural Steel 37Cr4/42CrV6–case-hardened
			Alloy Structural Steel 42CrV6– gear teeth case-hardened
			Alloy Structural Steel 37Cr4–gear teeth surface nitride
			Carbon Structural Steel Ck10/Ck15–case-hardened
			Carbon Structural Steel Ck50–case-hardened
			Carbon Structural Steel Ck60–hardened by nitriding
			Alloy Structural Steel 37Cr4–case-hardened
F	High	Large	Alloy Structural Steel 37Cr4/42CrV6–gear teeth case-hardened
			Alloy Structural Steel 34CrNiMo6–case-hardened
			Alloy Structural Steel 42MnV7/30CrV9/30CrMoV9/34CrNiMo6–nitride
G	Very High		Alloy Structural Steel 16MnCr5/35CrMo4–case-hardened
			Alloy Structural Steel 15NiCr6/14NiCr14–case-hardened
H	High Speed		Alloy Structural Steel 30CrV9/30CrMoV9/34CrNiMo6–nitrided

Diametral Pitch: The ratio of the number of teeth to the pitch diameter in inches. Unless otherwise specified, the transverse diametral pitch (specified in the transverse plane) is implied. For hypoid gears, it is the transverse diametral pitch of the gear member (Whitmire, 2003).

Pressure Angle: The angle at the pitch point between a line normal to the tooth profile and the pitch plane. See Figure 3.3. Unless otherwise specified for bevel and hypoid gears, the normal pressure angle (measured in the normal plane at the mean point) is implied. The normal pressure angle is that angle in the normal plane at the pitch point between the tangent plane and a radial line to the gear center. On most types of gears the pressure angles on both sides of the gear tooth profile are equal. An exception to this is in designs of gears with buttress teeth, such as hypoids. Hypoid gear teeth, because of their asymmetric relationship, do not naturally have equal pressure angles on their two sides. With spiral bevel gears, the designer may deliberately unbalance the pressure angles to produce a buttressed tooth. On spiral bevel and hypoid gears, the teeth are cut with lengthwise curvature. One tooth surface is concave; the other is convex. These two terms are used to identify the two sides of the gear teeth as seen from Figure 3.2 (Whitmire, 2003).

Spiral Angle: The angle between the tooth trace and an element of the pitch cone (Figure 3.2). The spiral angle is at the mean point, unless otherwise specified. On hypoid gears, the spiral angles on gear and mating pinion are unequal (Whitmire, 2003).

Module (Metric): The ratio of the pitch diameter in millimeters to the number of teeth. Unless otherwise specified, the transverse module (specified in the transverse plane) is implied. For hypoid gears, it is the transverse module of the gear member (Whitmire, 2003).

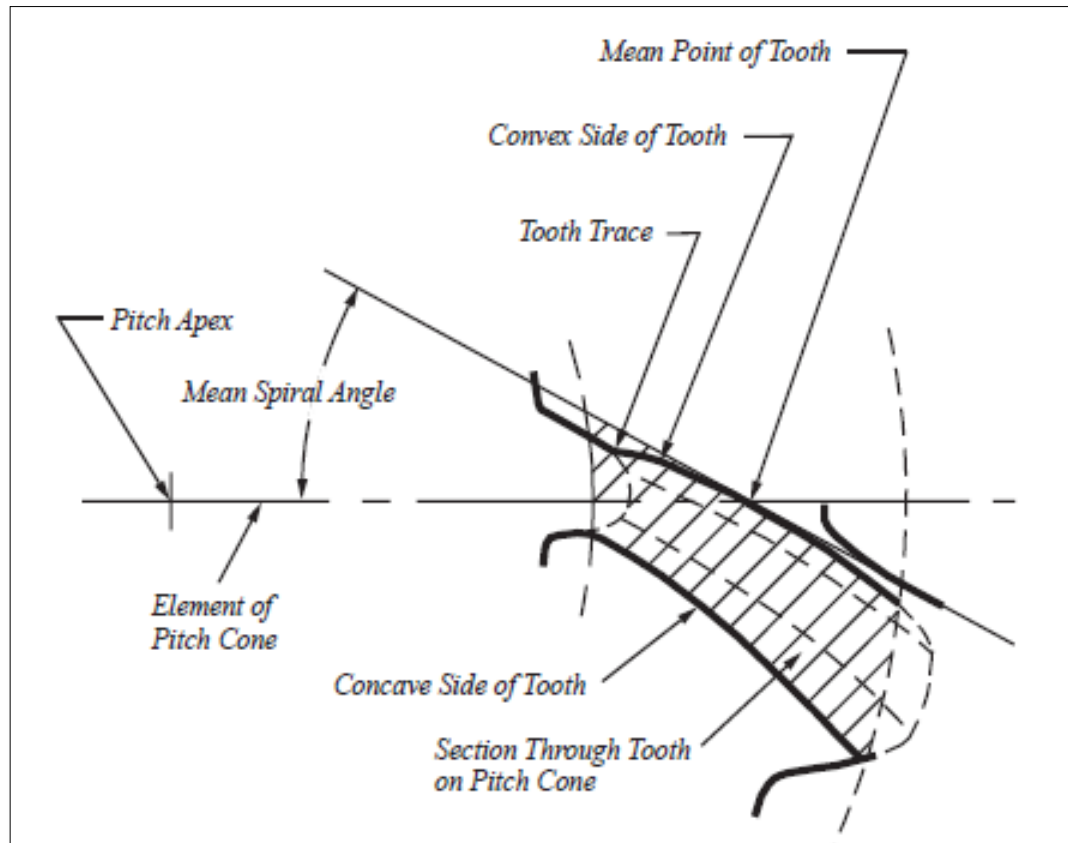


Fig.3.2 Mean Spiral Angle (Whitmire, 2003).

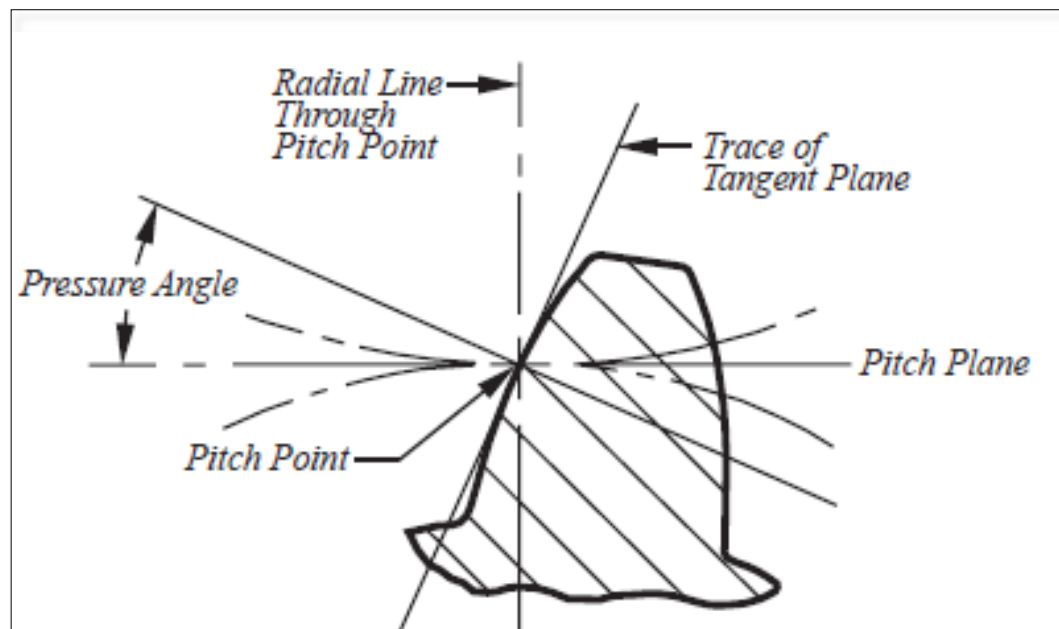


Figure 3.3 Pressure Angle (Whitmire, 2003).

In this study, various gear groups have been designed in order to determine the proper gear group for the spiral bevel gears of differential of the vehicle. Then, different gear systems have been modeled changing only the spiral angle (radius, conversion rate, number of teeth etc. are identical).

The gear designs in this study, has been first generated by Camnetics GearTeq Program, then, Solidworks has been used in order to establish arrangements and positioning required for the analysis of the system. Afterward, with the aid of ANSYS Commercial Software, material properties have been specified and the boundary conditions and loads have been applied.

Table 3.4 Dimension of Spiral Bevel Ring Gear

	System 1	System 2	System 3	System 4
Spiral Angle	0°	25°	34°	43°
Circular Pitch (mm)	25,133	25,133	25,133	25,133
Modular	8	8	8	8
Angles Sum of Pitch	90°	90°	90°	90°
Diameter Pitch (mm)	232	232	232	232
Number of Teeth	29	29	29	29
Pressure Angle	20°	20°	20°	20°

Table 3.5 Dimension of Spiral Bevel Pinion Gear

	System 1	System 2	System 3	System 4
Spiral Angle	0°	25°	34°	43°
Circular Pitch (mm)	25,133	25,133	25,133	25,133
Modular	8	8	8	8
Angles Sum of Pitch	90°	90°	90°	90°
Diameter Pitch (mm)	136	136	136	136
Number of Teeth	17	17	17	17
Pressure Angle	20°	20°	20°	20°

Dimensions of the gear groups modeled are shown in Table 3.4 and Table 3.5. As seen from Table 3.4 and Table 3.5, only the variation of the spiral angles has been examined. However, due to the straight bevel gear and spiral bevel gear manufacturing and design, there are very little differences between gear teeth thicknesses.

3.1.4 Modeling

In this part, the modeling phases of one of the gear systems used in the analysis are explained. The phases for the other gear systems are the same as well. Modeling has been carried out using Gearteq program.

The types of the gear modeled have been chosen from the menu above in GearTeq. Then, the program opens a dialogue box for the necessary data input. In this thesis, drawing of the gears used in System 3 will be explained. We have drawn the spiral bevel ring gear first, and then the spiral bevel pinion gear. Hence, the values for the spiral bevel ring gear are entered first (Figure 3.4). After the values are entered, the program shows the illustration for the spiral bevel ring gear. Later on, after choosing bevel gear option again, the program automatically forms a second gear that is compatible with the first (tooth type, spiral angle, module count etc). Changing the dimensions of the second gear (entering the spiral bevel pinion gear's measurements), we model the gear system desired (Figure 3.5).

After these processes have finished, the gear group has been transferred to SolidWorks program. Using SolidWorks, possible problems within the teeth (conflicts etc) have been controlled and starting positions of the gears have been adjusted for analysis. (Figure 3.6) If there is any problem, they are fixed after controlling the gears' positions or tooth profile lines.

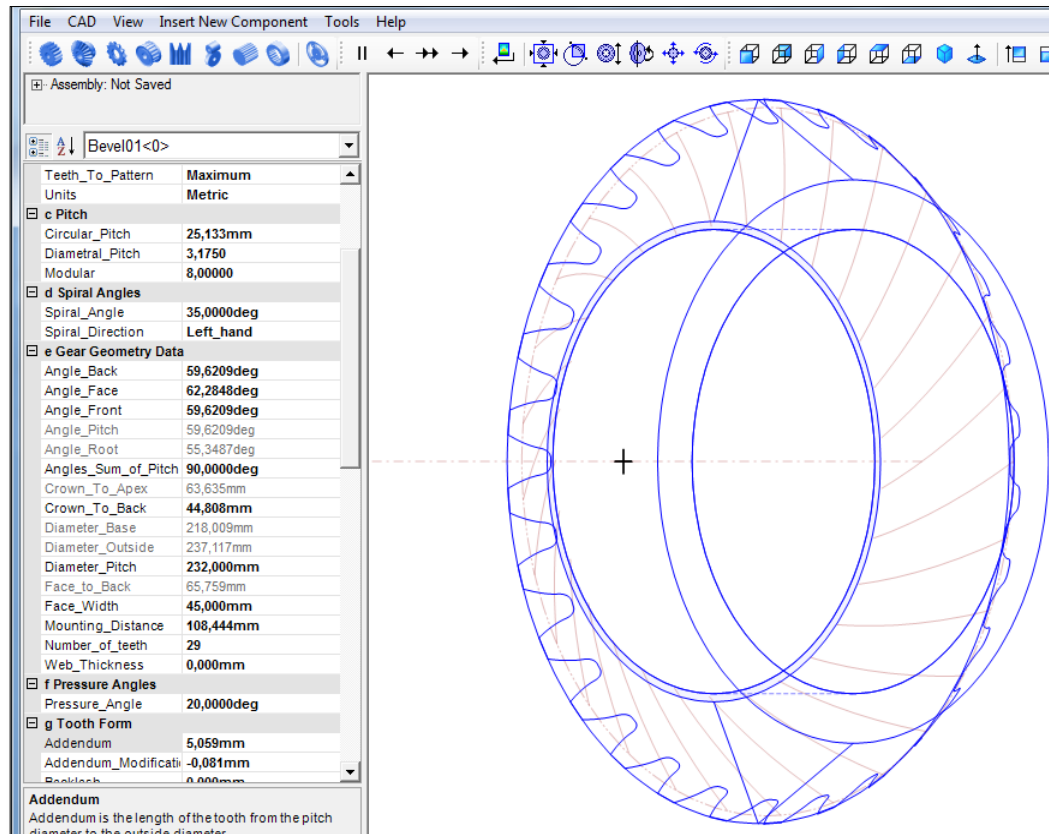


Figure 3.4 Modelling of the spiral bevel ring gear using GearTeq by entering its measurements

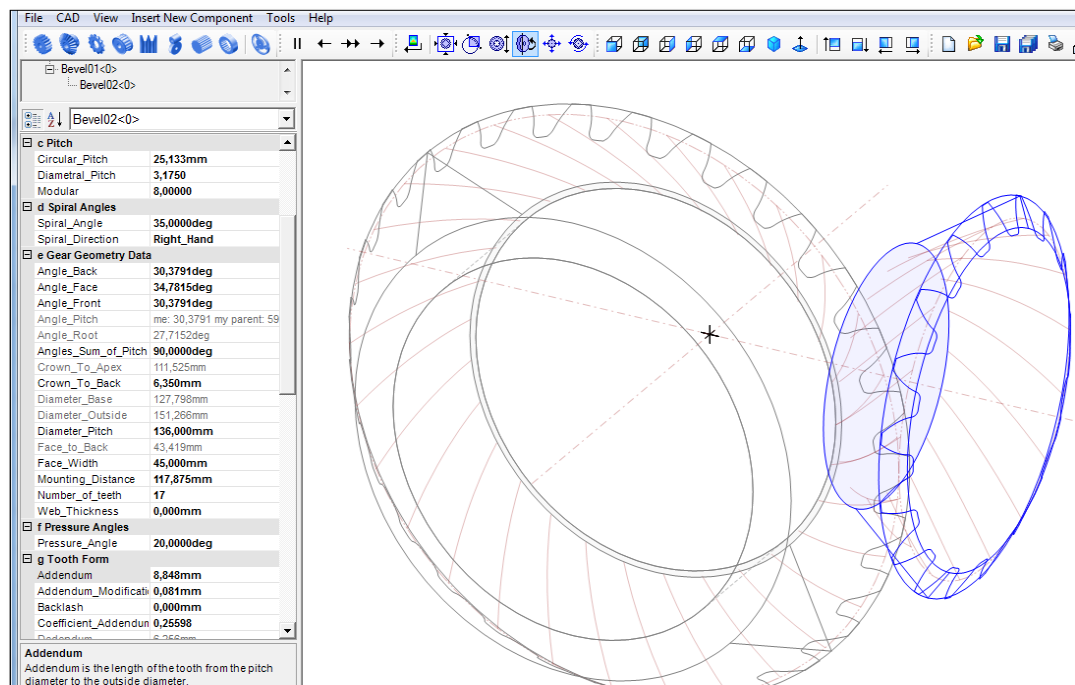


Figure 3.5 Forming the gear system using Gearteq

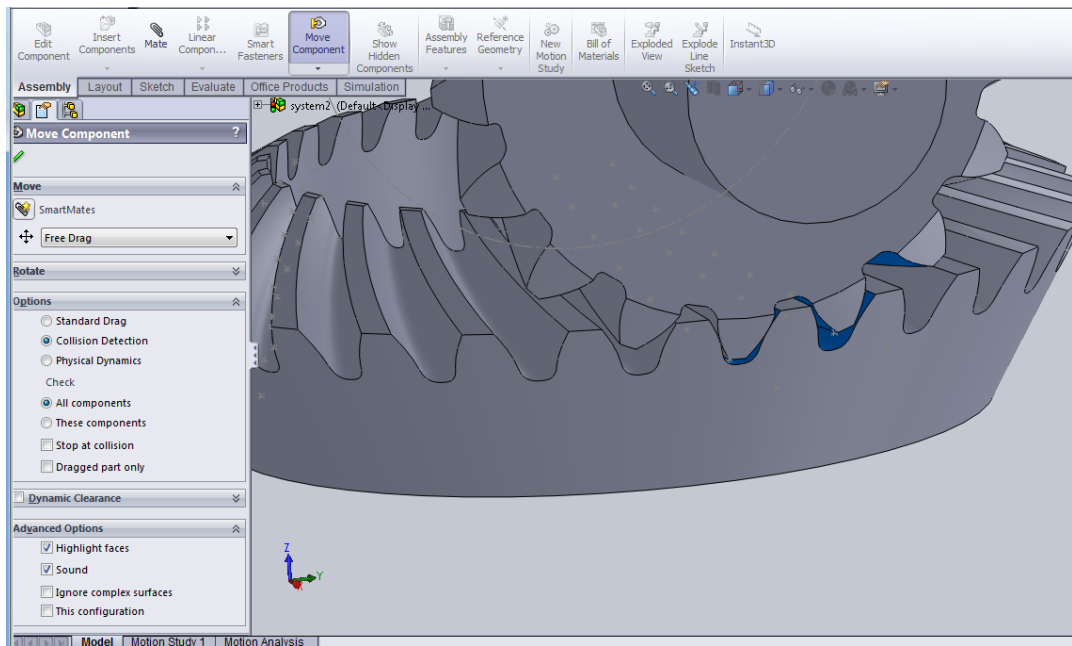


Figure 3.6 System control using SolidWorks

CHAPTER FOUR

FINITE ELEMENT ANALYSIS

In this chapter, the gears modeled have been analyzed by using the finite element method. Since spiral bevel gears have dimensions on all three-axes and spiral bevel gears that work together are exposed to loads from various directions, these analyses have to be three-dimensional.

If the boundary conditions and loads are defined correctly, the results of the finite element method implementation are predictable.

4.1 Finite Element Method

Today, the lengthy calculations of the classical methods have been replaced by computer-aided analysis. As the technology advanced, many important gains in terms of cost and time have arisen for manufacturing and design. Finite element method is the most used technique in computer-aided calculations.

The finite element method is a numerical analysis technique for obtaining approximate solutions to a wide variety of engineering problems. Although originally developed to study stress in complex airframe structures, it has since been extended and applied to the broad field of continuum mechanics. Because of its diversity and flexibility as an analysis tool, it is receiving much attention in engineering schools industry (Huebner, Dewhirst, Smith & Byrom, 2001).

In practice, a finite element analysis usually consists of three principal steps:

1. Preprocessing: The user constructs a model of the part to be analyzed in which the geometry is divided into a number of discrete sub-regions, or "elements," connected at discrete points called "nodes." Certain of these nodes will have fixed displacements, and others will have prescribed loads. These models can be extremely time consuming to prepare, and commercial codes vie with one another to have the most user-friendly graphical "preprocessor" to assist in this

rather tedious chore. Some of these preprocessors can overlay a mesh on a preexisting CAD file, so that finite element analysis can be done conveniently as part of the computerized drafting-and-design process.

2. Analysis: The dataset prepared by the preprocessor is used as input to the finite element code itself, which constructs and solves a system of linear or nonlinear algebraic equations

$$[K_{ij}]\{u_j\} = \{f_i\}$$

where u and f are the displacements and externally applied forces at the nodal points, respectively. The formation of the K matrix is dependent on the type of problem being attacked, and this module will outline the approach for truss and linear elastic stress analyses. Commercial codes may have very large element libraries, with elements appropriate to a wide range of problem types. One of FEA's principal advantages is that many problem types can be addressed with the same code, merely by specifying the appropriate element types from the library.

3. Postprocessing: In the earlier days of finite element analysis, the user would pore through reams of numbers generated by the code, listing displacements and stresses at discrete positions within the model. It is easy to miss important trends and hot spots this way, and modern codes use graphical displays to assist in visualizing the results. A typical postprocessor display overlays colored contours representing stress levels on the model, showing a full-filled picture similar to that of photoelastic or experimental results (Roylance, 2001).

Finite element method gives very realistic results, but for accurate results boundary conditions should be specified correctly. However, only specifying boundary conditions right is not enough. Mesh form and size should be chosen accurately as well. The smaller the mesh sizes are, the closer the results will be to reality. On the other hand, as the mesh size gets smaller, the processing time extends, and depending on the computer's memory, it may not perform processes over a certain number of mesh. Thus, in the analysis of complex drawings by finite element method, some techniques like symmetrical partitioning or dividing the important

areas into smaller meshes are applied. Nevertheless, due to the advanced computing technology today, drawings that are not too big or complex can be processed after being divided into sufficiently small meshes.

To perform an analysis using the finite element method the first step is to subdivide the region of interest into elements and nodes. In this process the analyst must make a choice on:

1. The type of elements to use;
2. Where to place nodes;
3. How to apply the loading and boundary restraints;
4. The appropriate material model and parameters values for each element;
5. Any other aspects relating to the particular problem.

The specification of the node and element data defines what we will subsequently refer to as the finite element mesh or, for short, the mesh of the problem (Taylor, 2011).

Two fundamental approaches have been pursued and refined, namely methods based on advancing front methodologies that generate elements from the boundary inwards and methods based on Delaunay triangularizations that directly mesh from coarse to fine over the complete domain. Although a large effort has already been expended on the development of effective mesh generation schemes, improvements still are much desired, for example to reach more general and effective procedures to mesh arbitrary three-dimensional geometries with brick elements (Bathe, 2009).

Figure 4.1 shows a three-dimensional mapped mesh of brick elements, a largely structured mesh, for the analysis of a wheel, and Fig. 4.2 shows a three-dimensional mesh of tetrahedral elements, an unstructured mesh, for the analysis of a helmet. It is important to be able to achieve the grading in elements shown in Fig. 4.2 because the potential area of contact on the helmet requires a fine mesh (Bathe, 2009).

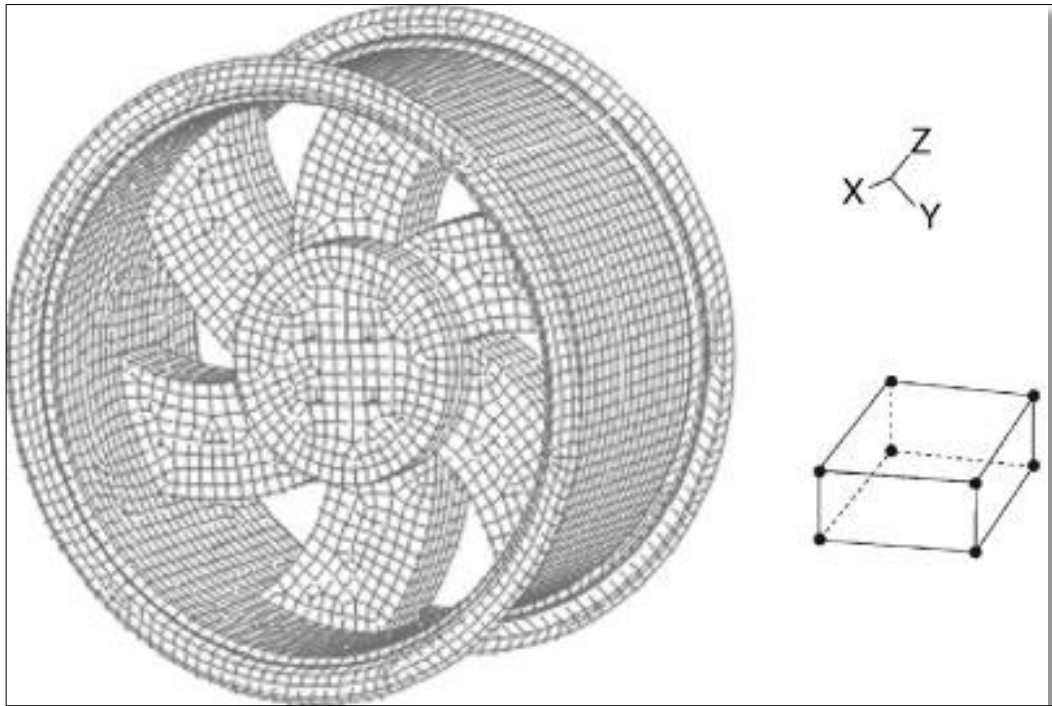


Figure 4.1. Finite element model of a wheel using three-dimensional brick elements, and a typical 8-node brick element ($q=8$) (Bathe, 2009).

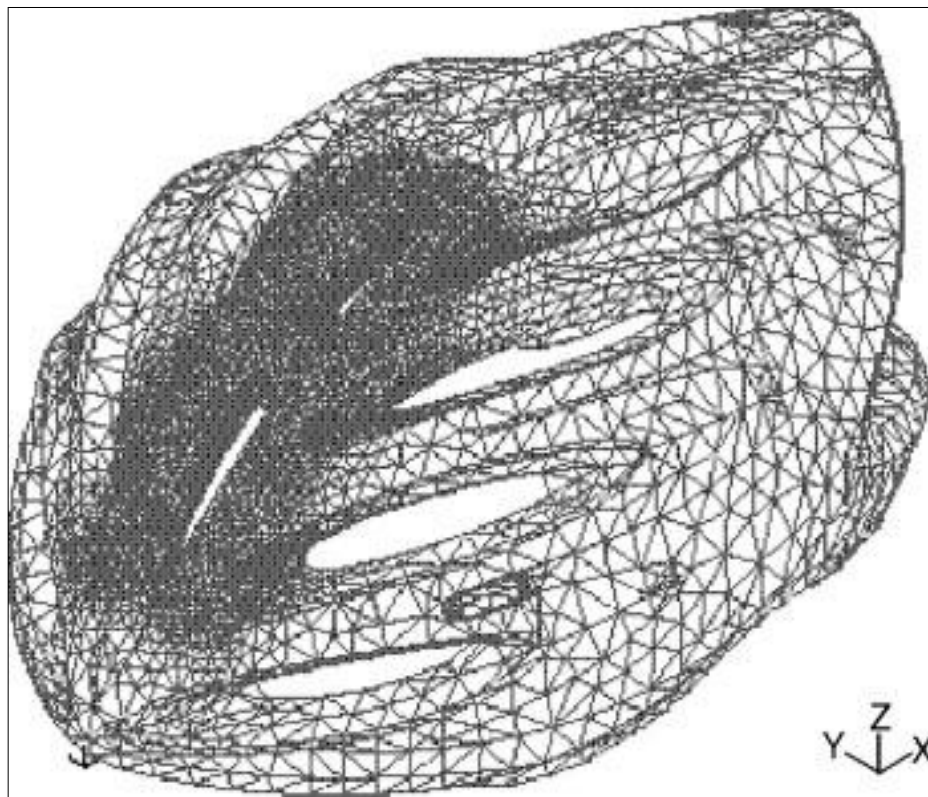


Figure 4.2 Model of a bicycle helmet showing mesh gradation (Bathe, 2009).

4.2 Analysis Phases

In this part, the analysis phases of the gear systems modeled using Ansys 12.1 Workbench have been explained. The analyses of four different gear systems, which were generated three-dimensionally using GearTeq software and SolidWorks, have been performed and the results have been examined and compared to the results in the literature.

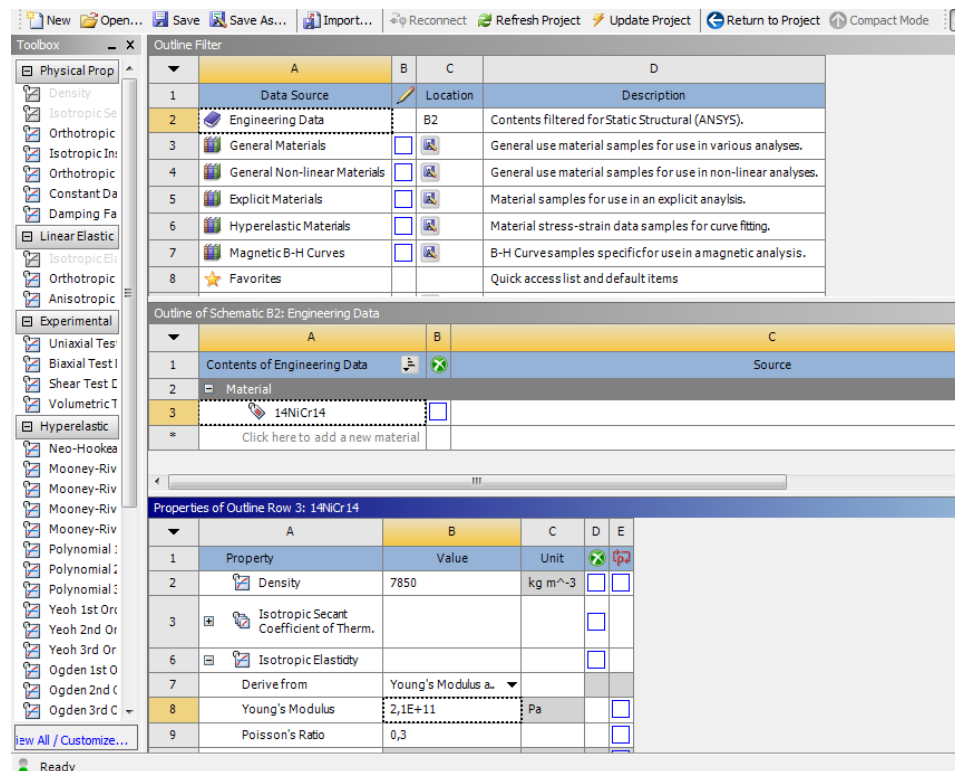


Figure 4.3 Material properties input

The three-dimensional models have been transferred from SolidWorks to Ansys for the contact analyses. Firstly, the analysis type has been chosen as static structural, and material properties given in Table 3.2 has been entered (Figure 4.3).

Subsequently, model screen for the analysis has been opened. In the model screen, materials' statuses, mesh, loads, boundary conditions and the results have been specified. Actually, the full analysis and results are both displayed on this screen. After checking the contact region and then meshing, boundary conditions have been

defined. We can determine the status of the main area more accurately, by dividing the contact region to smaller elements (Figure 4.4). Afterward, the loading type has been chosen and the torque of 6500 Nm that we had calculated using the data in Table 3.1 has been entered.

Boundary conditions and torque have been specified accordingly to the working conditions planned (Figure 4.5). Since this study is based on the torques of the gears relative to each other, spiral bevel ring gear was accepted as stable and only the spiral bevel pinion gear was allowed to rotate.

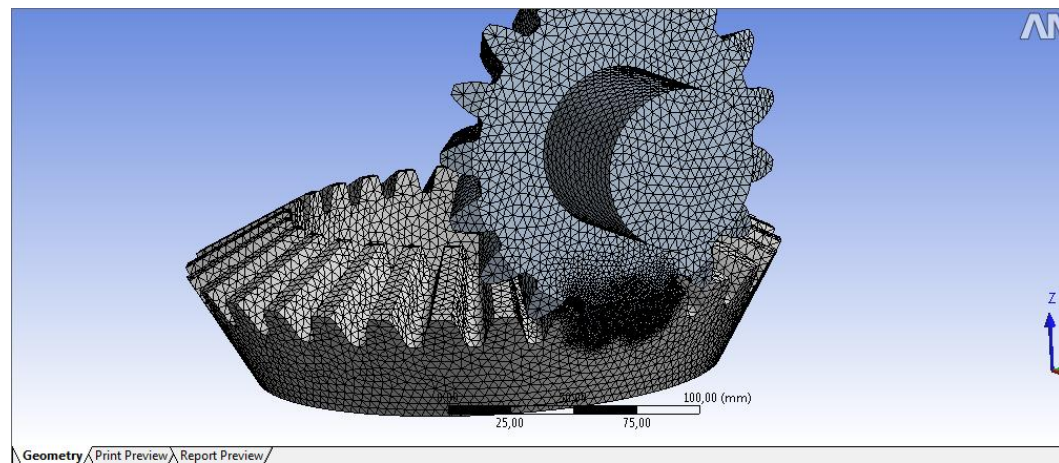


Figure 4.4 Finite element model of the gear system

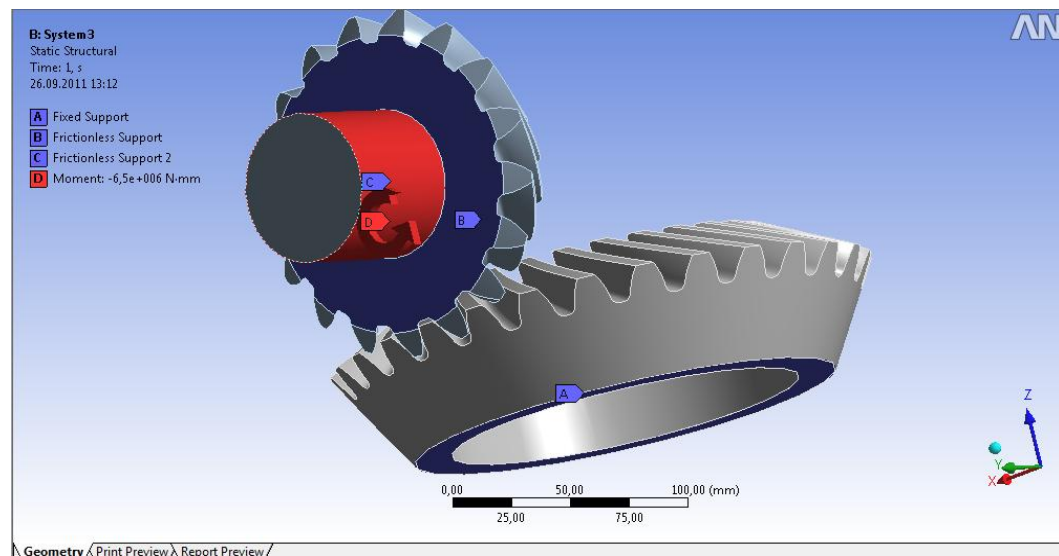


Figure 4.5 Boundary conditions and loading

After the boundary conditions have been defined, the types of analysis results desired to determine have been chosen and the program has been start solving (Figure 4.6). In this study deformation, strain and stress values have been obtained to determine the effect of the spiral angle.

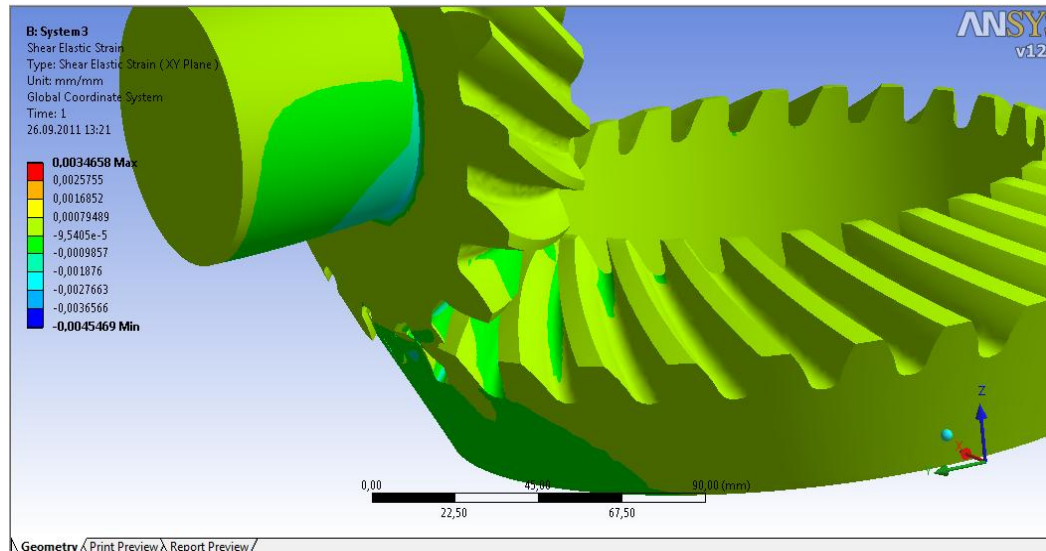


Figure 4.6 Analysis results screen

Analysis results are displayed as modal and numerical on the screen as seen from Figure 4.6. In addition, ANSYS Software offers the report as a print out.

4.3 Analysis Results

In this part, analysis results of the four different gear groups have been compared to each other. The effect of spiral angle variation of the gears has been observed.

Strain, stress and deformation distribution on both the spiral bevel ring gear and pinion gear results have been examined.

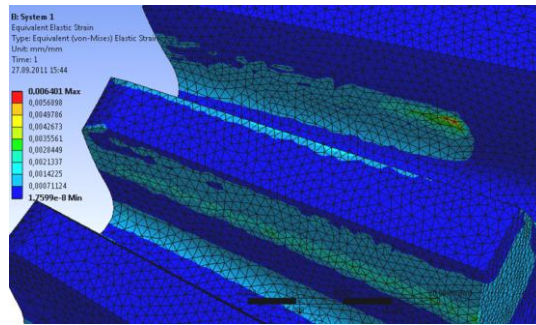
4.3.1 Strains

As seen from comparison graphs of the strain results, strains have increased for the spiral angles until 34^0 , for angles higher than 34^0 it has been observed that the

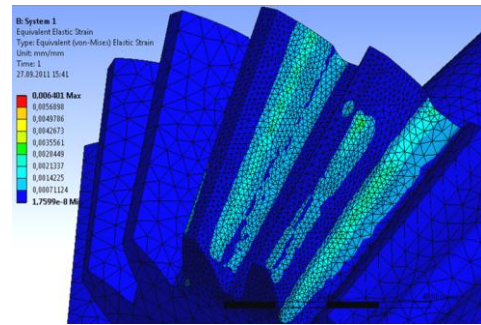
strain value decreases. It should be taken into account that only the analysis for up to a spiral angle of 43^0 has been made in this study.

Figures 4.7, Figure 4.8, Figure 4.9 ve Figure 4.10 show the equivalent (von-Mises) elastic strain distributions. Figure 4.12, Figure 4.13, Figure 4.14 and Figure 4.15 show the maximum principal elastic strain distribution. Figure 4.17, Figure 4.18, Figure 4.19 and Figure 4.20 show the maximum shear elastic strain distribution, and Figure 4.22, Figure 4.23, Figure 4.24 and Figure 4.25 show the normal elastic strain distribution.

4.3.1.1 Equivalent (von-Mises) Elastic Strain

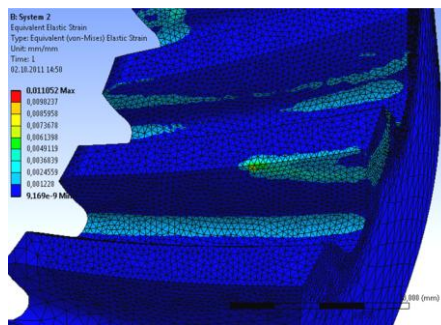


a. Spiral Bevel Ring Gear

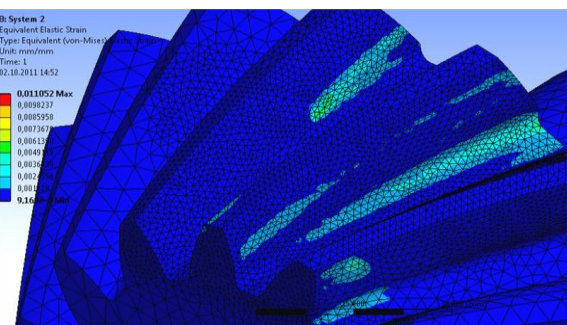


b. Spiral Bevel Pinion Gear

Figure 4.7 Equivalent (von-Mises) Elastic Strain Distribution for System 1

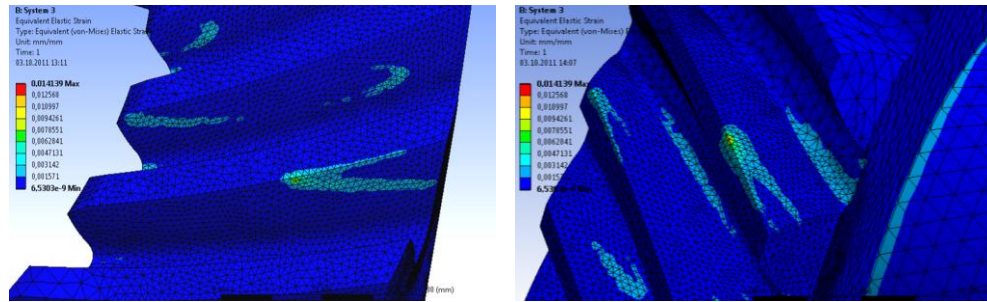


a. Spiral Bevel Ring Gear



b. Spiral Bevel Pinion Gear

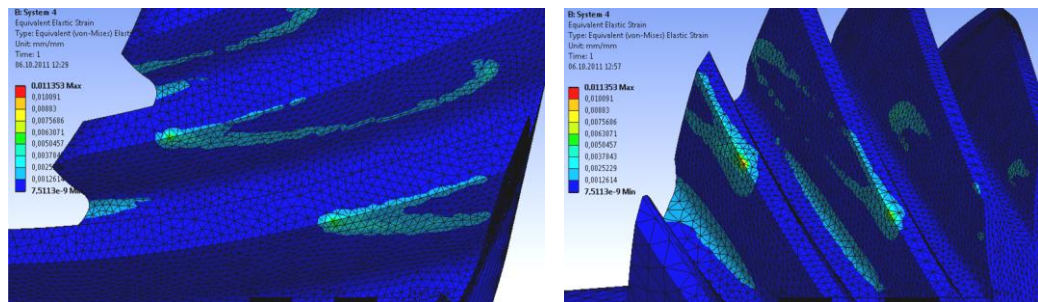
Figure 4.8 Equivalent (von-Mises) Elastic Strain Distribution for System 2



a. Spiral Bevel Ring Gear

b. Spiral Bevel Pinion Gear

Figure 4.9 Equivalent (von-Mises) Elastic Strain Distribution for System 3



a. Spiral Bevel Ring Gear

b. Spiral Bevel Pinion Gear

Figure 4.10 Equivalent (von-Mises) Elastic Strain Distribution for System 4

Table 4.1 Equivalent (von-Mises) Elastic Strain Comparison Table

Results	System 1	System 2	System 3	System 4
Minimum (-)	1,7599E-08	9,1690E-09	6,5303E-09	7,5113E-09
Maximum (-)	6,4010E-03	1,1052E-02	1,4139E-02	1,1353E-02
Minimum Occurs On	Bevel01-1	Bevel01-1	Bevel01-1	Bevel01-1
Maximum Occurs On	Bevel01-1	Bevel01-1	Bevel02-1	Bevel02-1

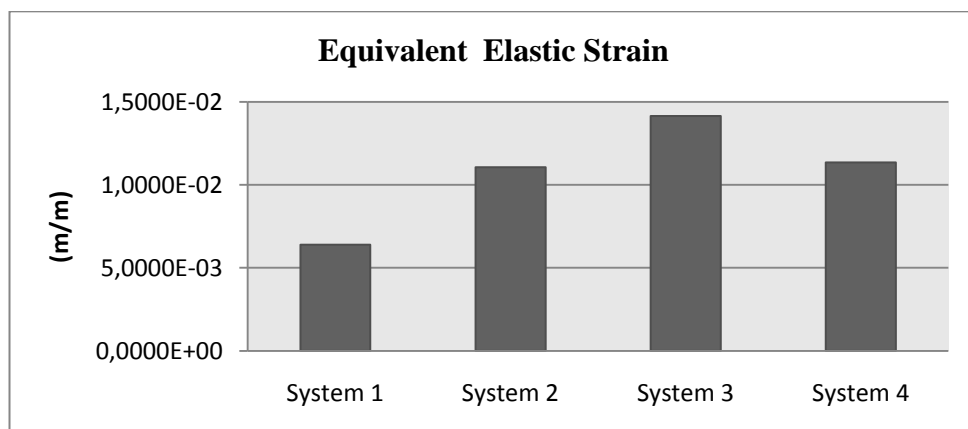
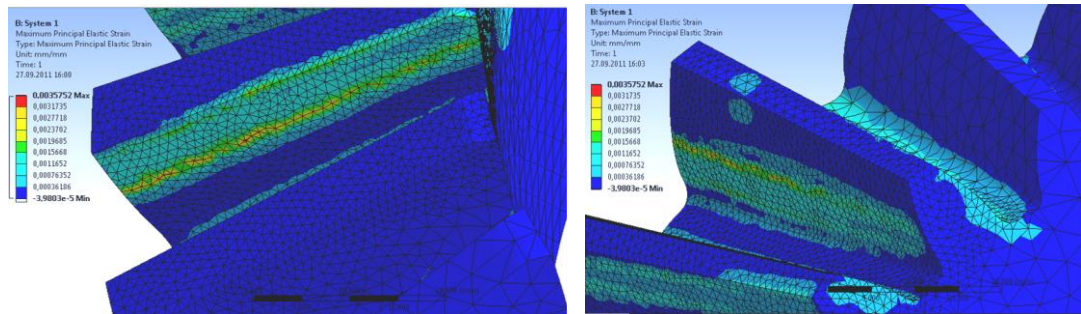


Figure 4.11 Variation of the Equivalent (von-Mises) Elastic Strain

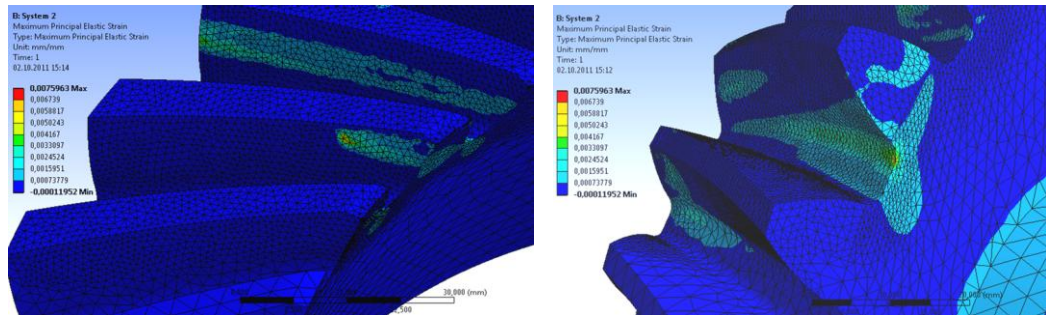
4.3.1.2 Maximum Principal Elastic Strain



a. Spiral Bevel Ring Gear

b. Spiral Bevel Pinion Gear

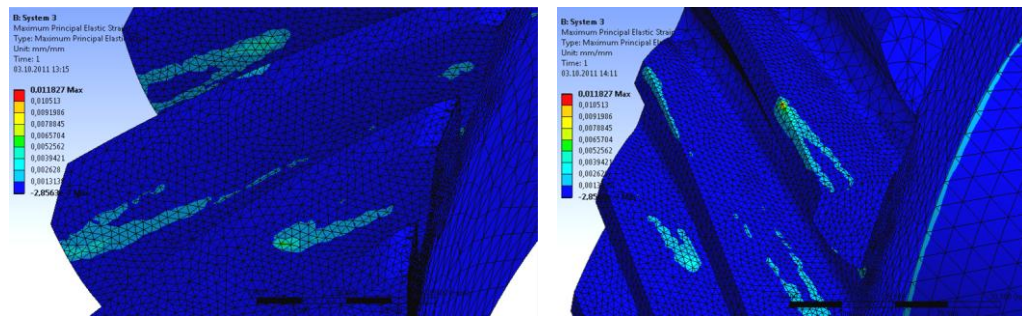
Figure 4.12 Maximum Principal Elastic Strain Distribution for System 1



a. Spiral Bevel Ring Gear

b. Spiral Bevel Pinion Gear

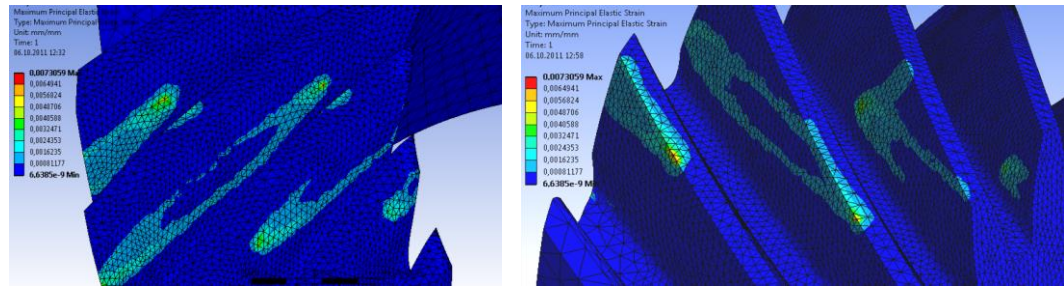
Figure 4.13 Maximum Principal Elastic Strain Distribution for System 2



a. Spiral Bevel Ring Gear

b. Spiral Bevel Pinion Gear

Figure 4.14 Maximum Principal Elastic Strain Distribution for System 3



a. Spiral Bevel Ring Gear

b. Spiral Bevel Pinion Gear

Figure 4.15 System 4 Maximum Principal Elastic Strain

Table 4.2 Comparison Table for Maximum Principal Elastic Strain

Results	<i>System 1</i>	<i>System 2</i>	<i>System 3</i>	<i>System 4</i>
Minimum (-)	-3,9803E-05	-1,1952E-04	-2,8563E-07	6,6385E-09
Maximum (-)	3,5752E-03	7,5963E-03	1,1827E-02	7,3059E-03
Minimum Occurs On	Bevel02-1	Bevel02-1	Bevel01-1	Bevel01-1
Maximum Occurs On	Bevel01-1	Bevel01-1	Bevel02-1	Bevel02-1

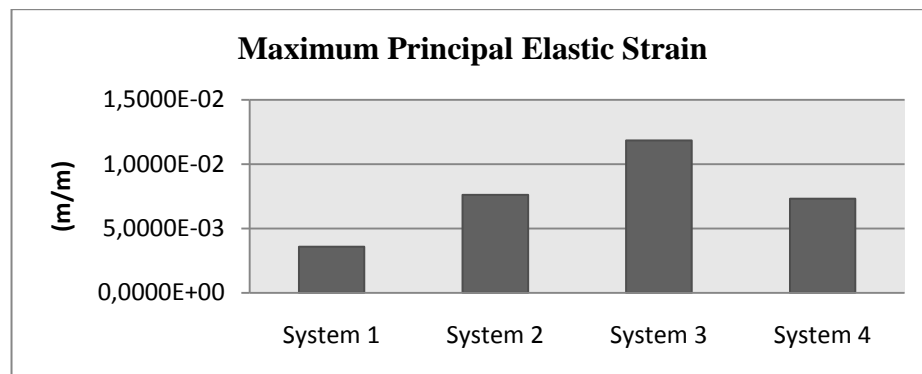
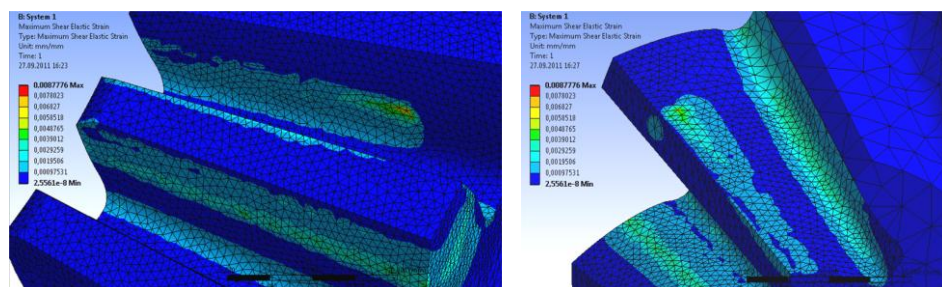


Figure 4.16 Variation of the Maximum Principal Elastic Strain

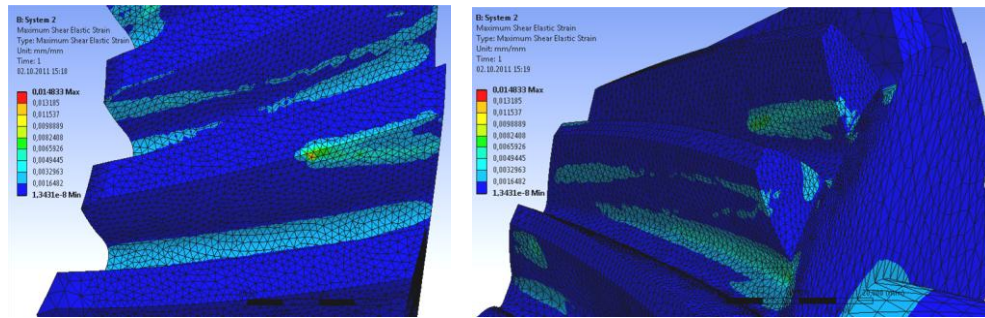
4.3.1.3 Maximum Shear Elastic Strain



a. Spiral Bevel Ring Gear

b. Spiral Bevel Pinion Gear

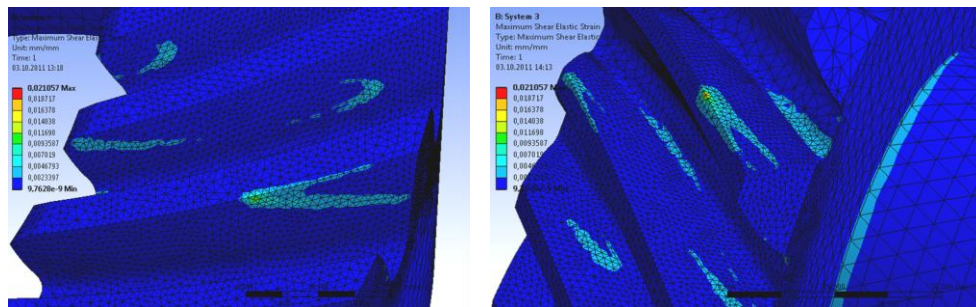
Figure 4.17 Maximum Shear Elastic Strain Distribution for System 1



a. Spiral Bevel Ring Gear

b. Spiral Bevel Pinion Gear

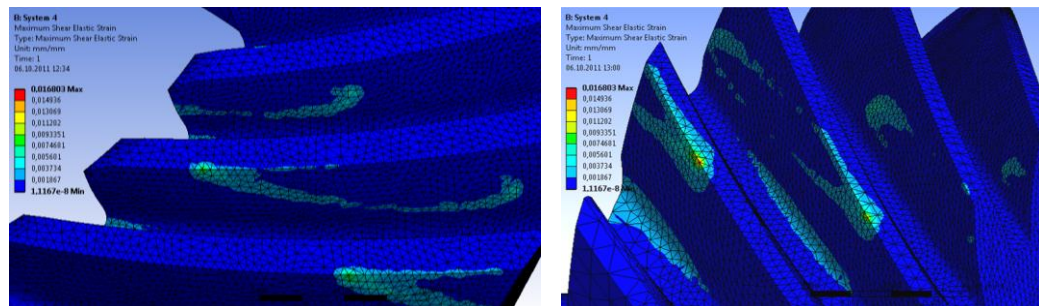
Figure 4.18 Maximum Shear Elastic Strain Distribution for System 2



a. Spiral Bevel Ring Gear

b. Spiral Bevel Pinion Gear

Figure 4.19 Maximum Shear Elastic Strain Distribution for System 3



a. Spiral Bevel Ring Gear

b. Spiral Bevel Pinion Gear

Figure 4.20 Maximum Shear Elastic Strain Distribution for System 4

Table 4.3 Comparison Table for Maximum Shear Elastic Strain

Results	System 1	System 2	System 3	System 4
Minimum (-)	2,5561E-08	1,3431E-08	9,7628E-09	1,1167E-08
Maximum (-)	8,7776E-03	1,4833E-02	2,1057E-02	1,6803E-02
Minimum Occurs On	Bevel01-1	Bevel01-1	Bevel01-1	Bevel01-1
Maximum Occurs On	Bevel01-1	Bevel01-1	Bevel02-1	Bevel02-1

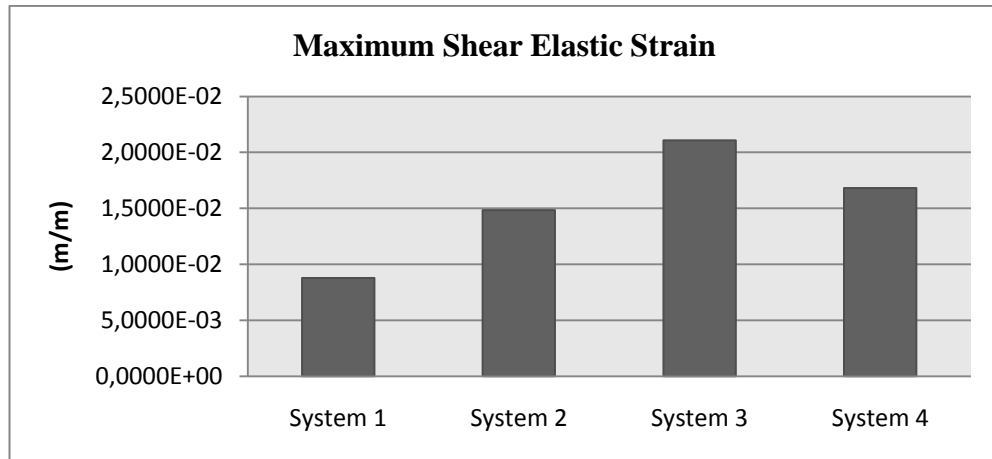
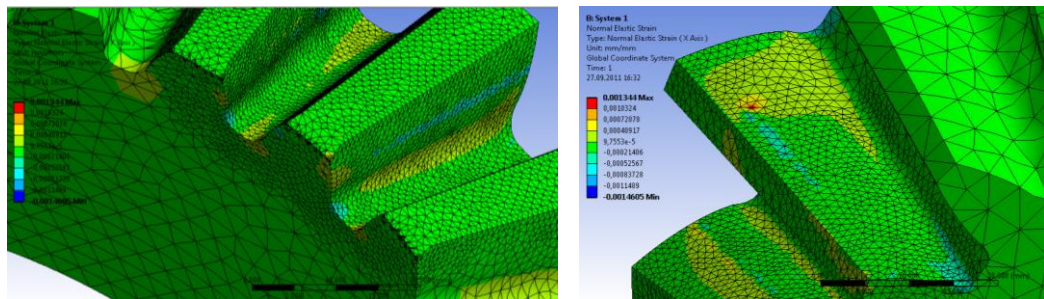


Figure 4.21 Variation of the Maximum Shear Elastic Strain

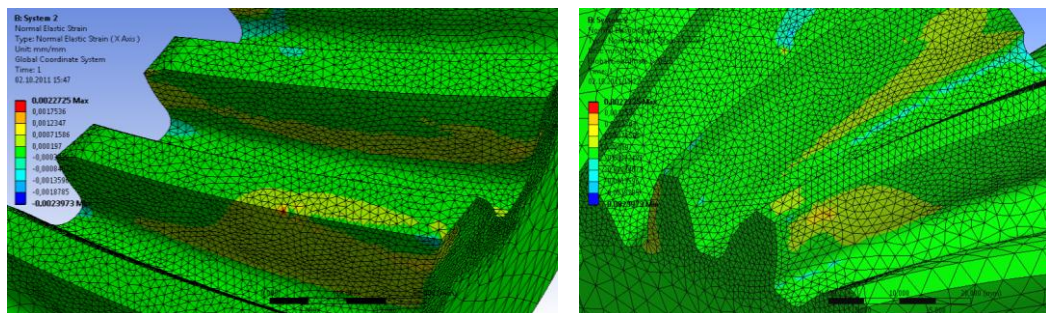
4.3.1.4 Normal Elastic Strain



a. Spiral Bevel Ring Gear

b. Spiral Bevel Pinion Gear

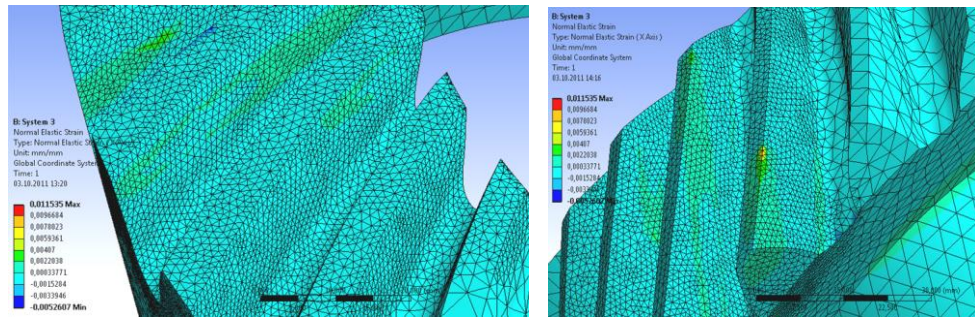
Figure 4.22 Normal Elastic Strain Distribution for System 1



a. Spiral Bevel Ring Gear

b. Spiral Bevel Pinion Gear

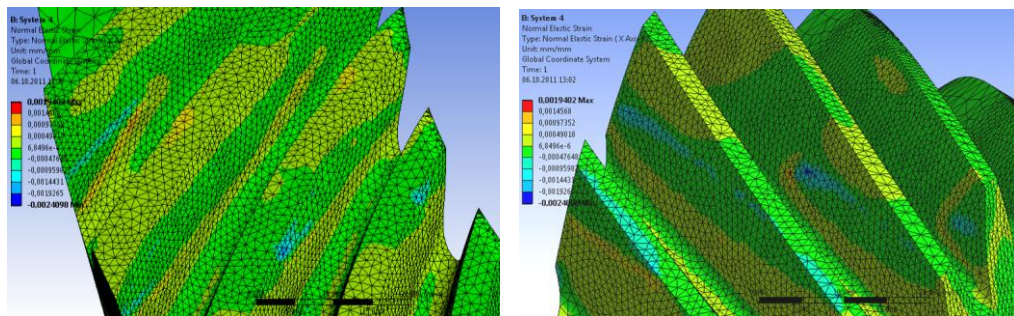
Figure 4.23 Normal Elastic Strain Distribution for System 2



a. Spiral Bevel Ring Gear

b. Spiral Bevel Pinion Gear

Figure 4.24 Normal Elastic Strain Distribution for System 3



a. Spiral Bevel Ring Gear

b. Spiral Bevel Pinion Gear

Figure 4.25 Normal Elastic Strain Distribution for System 4

Table 4.4 Comparison Table for Normal Elastic Strain

Results	System 1	System 2	System 3	System 4
Orientation	X Axis	X Axis	X Axis	X Axis
Minimum (-)	-1,4605E-03	-2,3973E-03	-5,2607E-03	-2,4098E-03
Maximum (-)	1,3440E-03	2,2725E-03	1,1535E-02	1,9402E-03
Minimum Occurs On	Bevel01-1	Bevel01-1	Bevel01-1	Bevel02-1
Maximum Occurs On	Bevel02-1	Bevel01-1	Bevel02-1	Bevel02-1

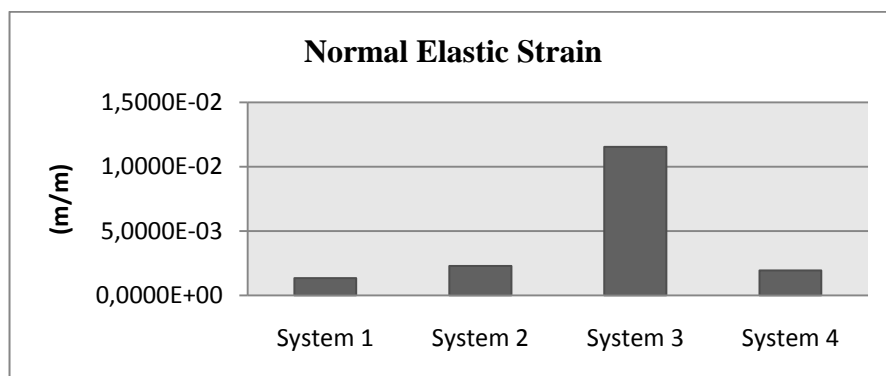


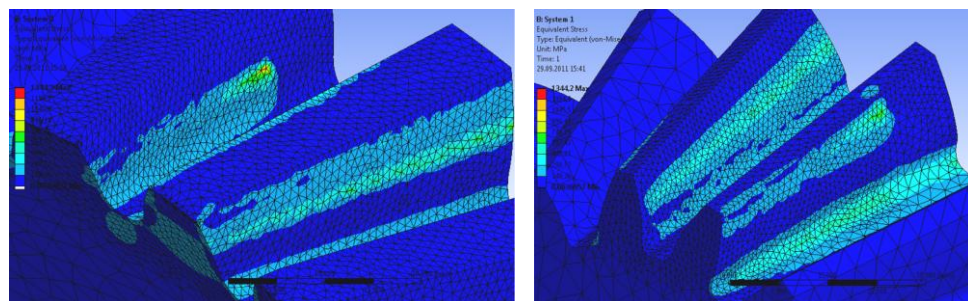
Figure 4.26 Variation of Normal Elastic Strain

4.3.2 Stresses

In this section, the effect of the spiral angles on the stress distributions on the gears has been investigated. As seen from Figures 4.27-30 and the graphs in Figure 4.31, as the spiral angle increases, so does the stress values at first and over 34° , the stresses begin to decrease.

Figure 4.27-4.30 show equivalent (von-Mises) stress distribution on the gears. Figure 4.32-4.35 show the maximum principal stress distribution. Figure 4.37-4.40 show the maximum shear stress distribution. Figure 4.42-4.45 show the normal stress distribution. As seen all these figures, local increase largely in the stress values has been observed. This is agree with the results of the studies in the literature. (eg. Litvin, Fuentes & Hayasaka, 2006). In addition, fractures in the gears occur in these regions as shown in Figure 4.47.

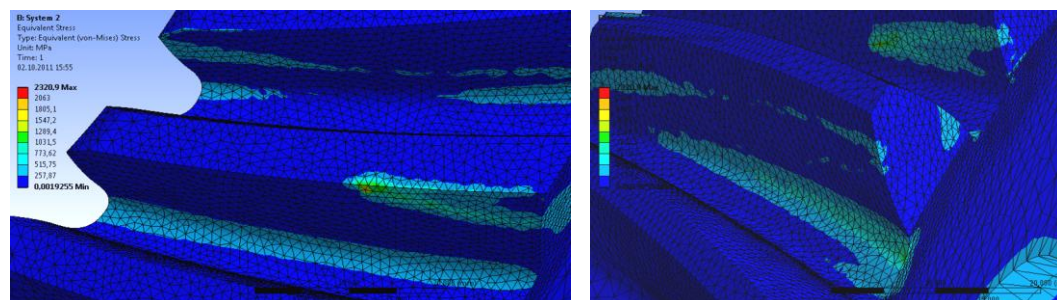
4.3.2.1 Equivalent Stress



a. Spiral Bevel Ring Gear

b. Spiral Bevel Pinion Gear

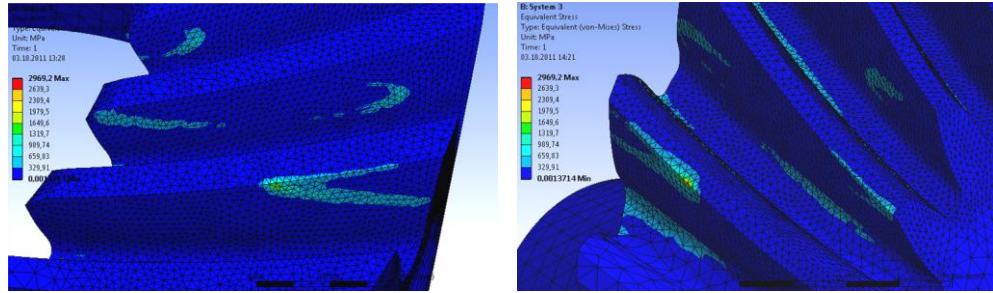
Figure 4.27 Equivalent Stress Distribution for System 1



a. Spiral Bevel Ring Gear

b. Spiral Bevel Pinion Gear

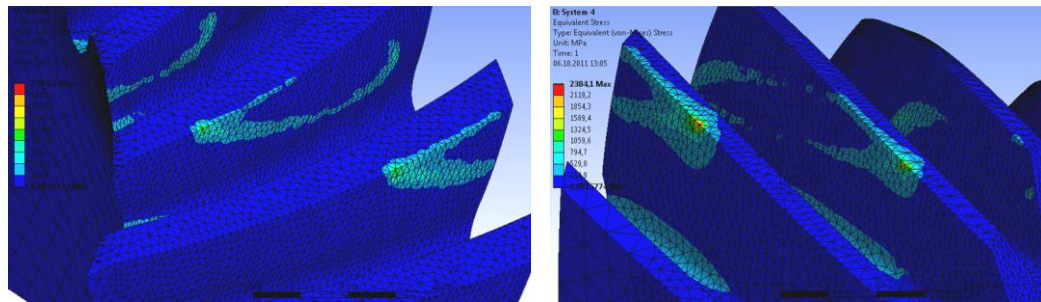
Figure 4.28 Equivalent Stress Distribution for System 2



a. Spiral Bevel Ring Gear

b. Spiral Bevel Pinion Gear

Figure 4.29 Equivalent Stress Distribution for System 3



a. Spiral Bevel Ring Gear

b. Spiral Bevel Pinion Gear

Figure 4.30 Equivalent Stress Distribution for System 4

Table 4.5 Comparison Table for Equivalent Stress

Results	System 1	System 2	System 3	System 4
Minimum (MPa)	3,6957E-03	1,9255E-03	1,3714E-03	1,5774E-03
Maximum (MPa)	1344.2	2320.9	2969.2	2384.1
Minimum Occurs On	Bevel01-1	Bevel01-1	Bevel01-1	Bevel01-1
Maximum Occurs On	Bevel01-1	Bevel01-1	Bevel02-1	Bevel02-1

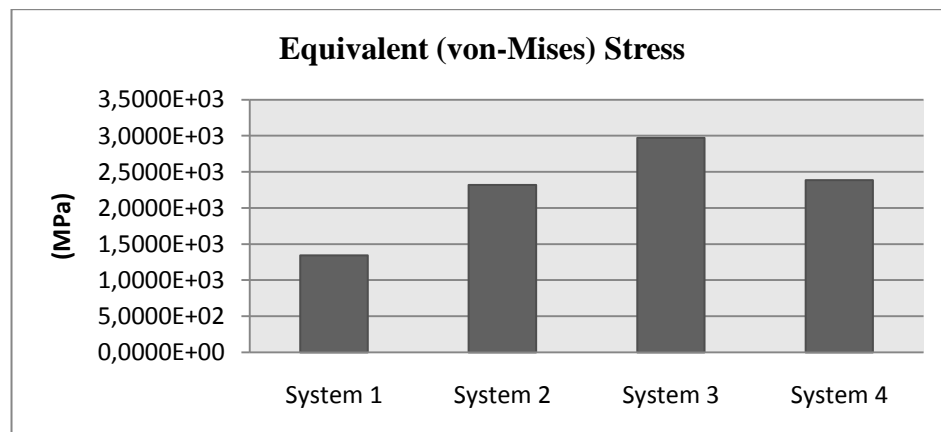
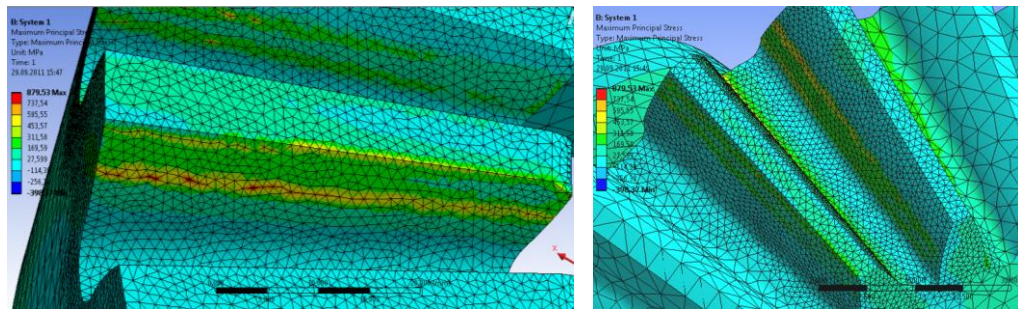


Figure 4.31 Equivalent Stress Change Graph

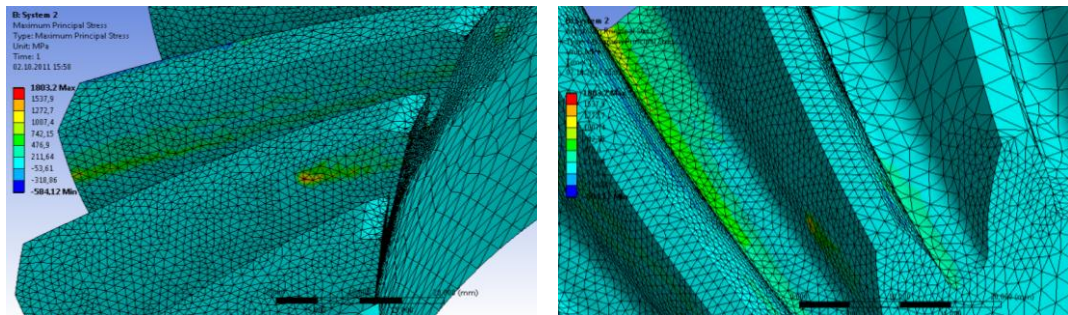
4.3.2.2 Maximum Principal Stress



a. Spiral Bevel Ring Gear

b. Spiral Bevel Pinion Gear

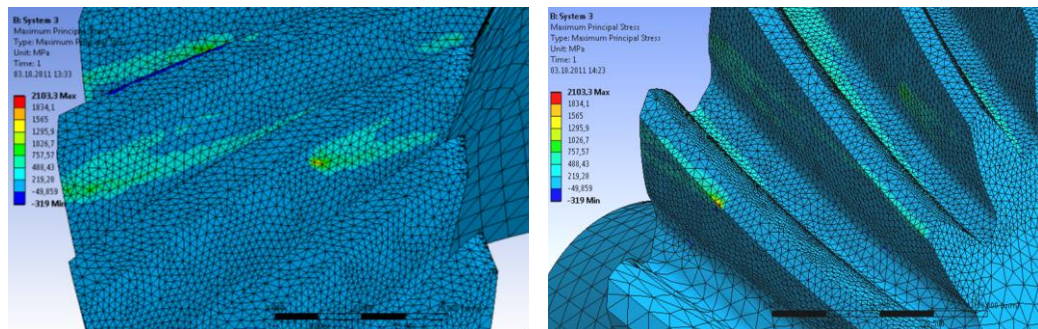
Figure 4.32 Maximum Principal Stress Distribution for System 1



a. Spiral Bevel Ring Gear

b. Spiral Bevel Pinion Gear

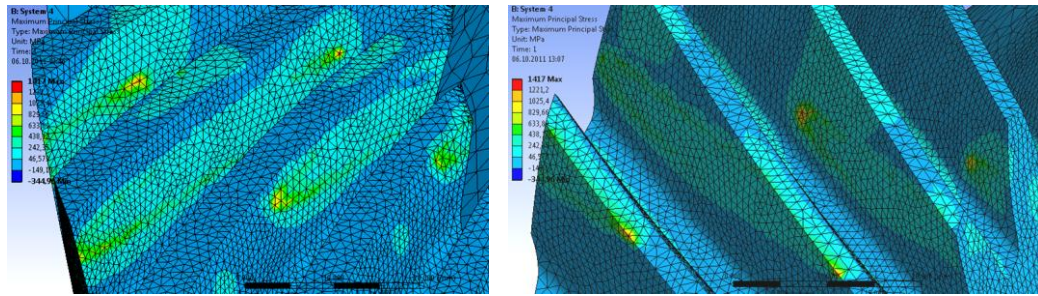
Figure 4.33 Maximum Principal Stress Distribution for System 2



a. Spiral Bevel Ring Gear

b. Spiral Bevel Pinion Gear

Figure 4.34 Maximum Principal Stress Distribution for System 3



a. Spiral Bevel Ring Gear

b. Spiral Bevel Pinion Gear

Figure 4.35 Maximum Principal Stress Distribution for System 4

Table 4.6 Maximum Principal Stress Comparison Table

Results	System 1	System 2	System 3	System 4
Minimum (MPa)	-3,9837E-02	-5,8412E-02	-3,1900E-02	-3,4496E-02
Maximum (MPa)	8795.3	1803.2	2103.3	1417.0
Minimum Occurs On	Bevel01-1	Bevel02-1	Bevel01-1	Bevel02-1
Maximum Occurs On	Bevel01-1	Bevel01-1	Bevel02-1	Bevel01-1

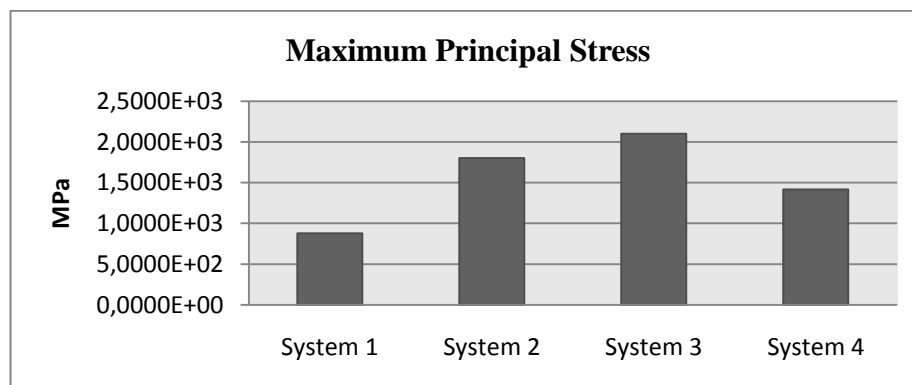
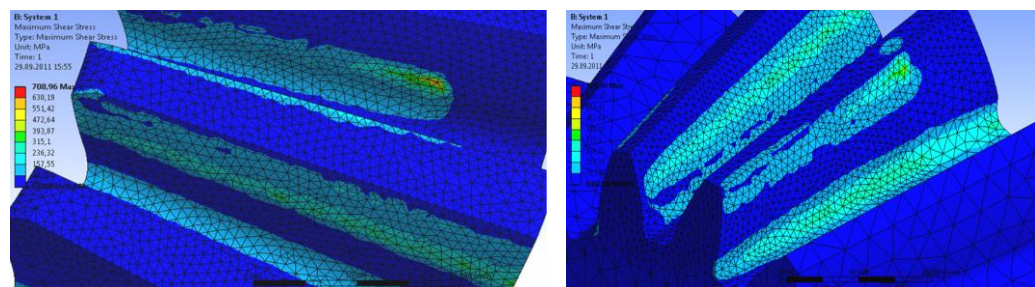


Figure 4.36 Maximum Principal Stress Change Graph

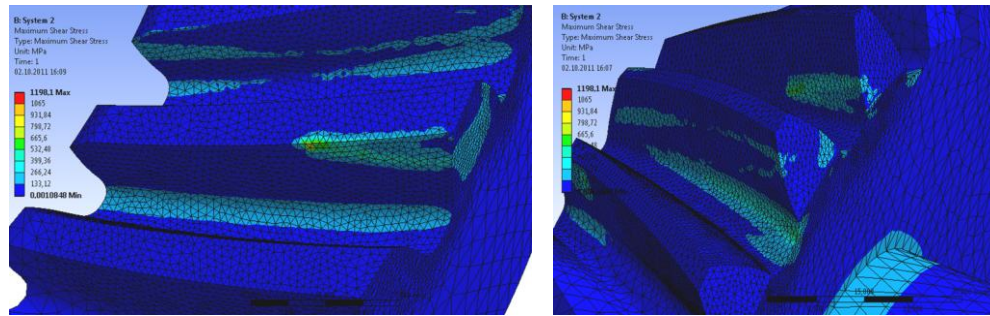
4.3.2.3 Maximum Shear Stress



a. Spiral Bevel Ring Gear

b. Spiral Bevel Pinion Gear

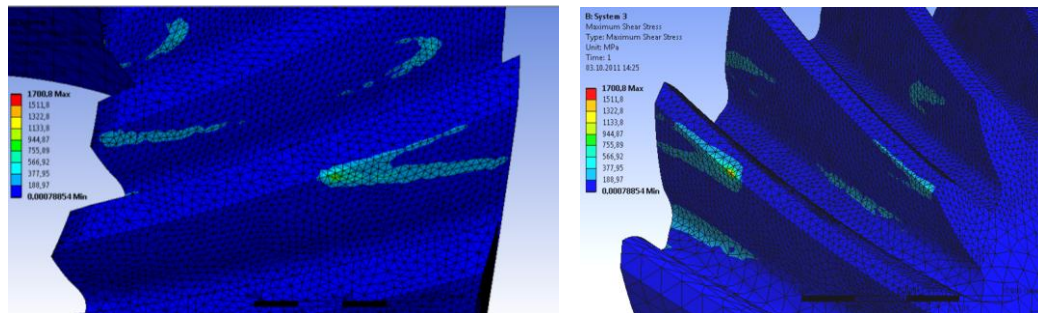
Figure 4.37 Maximum Shear Stress Distribution for System 1



a. Spiral Bevel Ring Gear

b. Spiral Bevel Pinion Gear

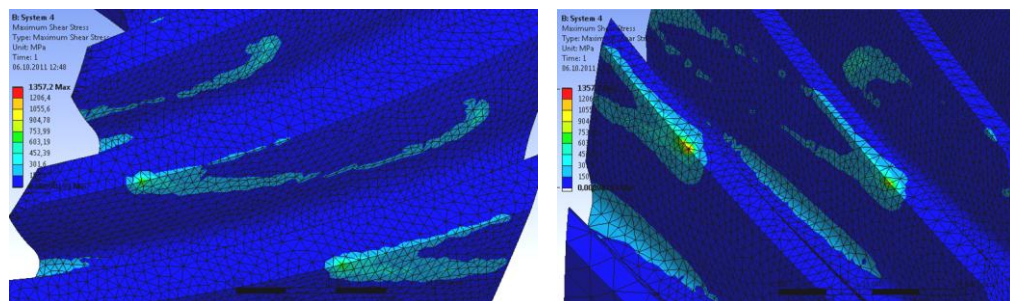
Figure 4.38 Maximum Shear Stress Distribution for System 2



a. Spiral Bevel Ring Gear

b. Spiral Bevel Pinion Gear

Figure 4.39 Maximum Shear Stress Distribution for System 3



a. Spiral Bevel Ring Gear

b. Spiral Bevel Pinion Gear

Figure 4.40 Maximum Shear Stress Distribution for System 4

Table 4.7 Comparison Table for Maximum Shear Stress

Results	<i>System 1</i>	<i>System 2</i>	<i>System 3</i>	<i>System 4</i>
Minimum (MPa)	2,0646E-03	1,0848E-03	0.78854E-03	0.90193E-03
Maximum (MPa)	708.96	1198.1	1700.8	1357.2
Minimum Occurs On	Bevel01-1	Bevel01-1	Bevel01-1	Bevel01-1
Maximum Occurs On	Bevel01-1	Bevel01-1	Bevel02-1	Bevel02-1

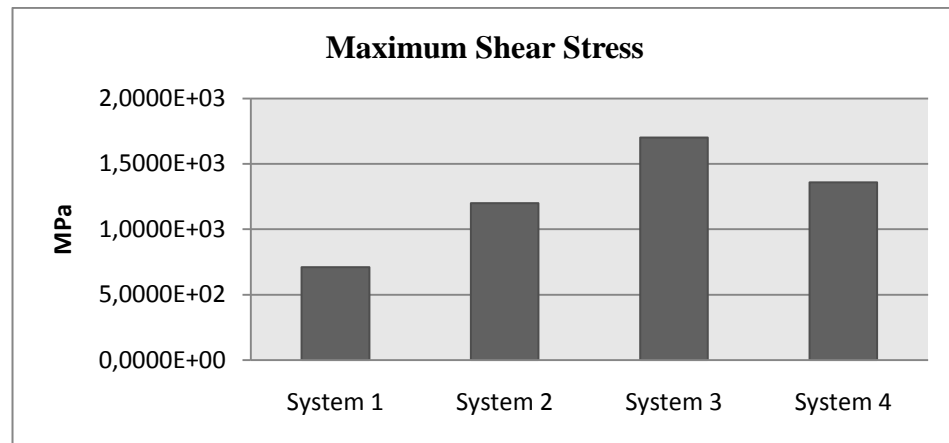


Figure 4.41 Variation of Maximum Shear Stress

4.3.2.4 Normal Stress

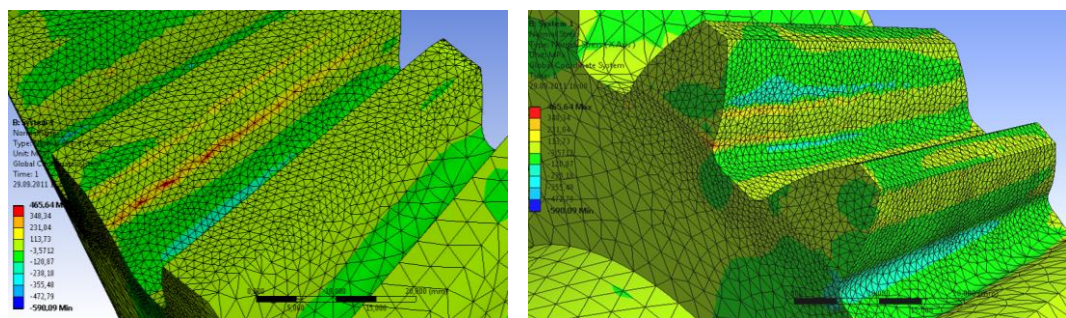


Figure 4.42 Normal Stress Distribution for System 1

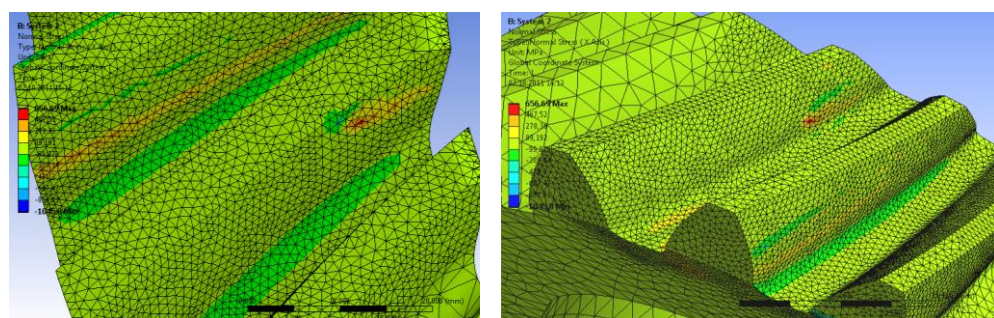
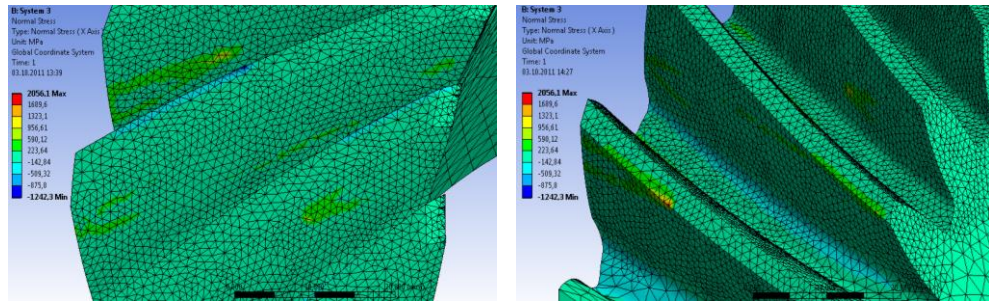


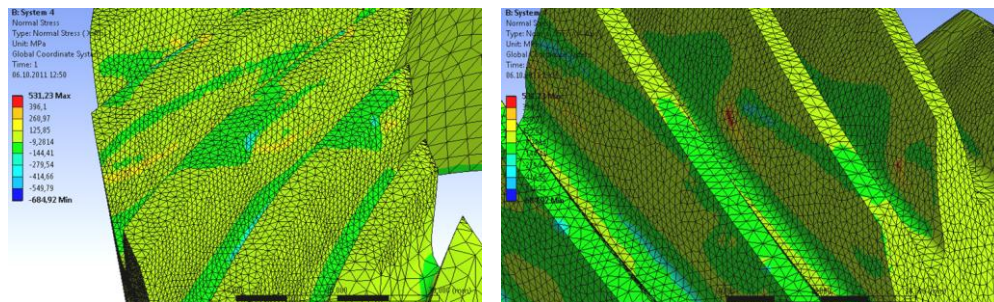
Figure 4.43 Normal Stress Distribution for System 2



a. Spiral Bevel Ring Gear

b. Spiral Bevel Pinion Gear

Figure 4.44 Normal Stress Distribution for System 3



a. Spiral Bevel Ring Gear

b. Spiral Bevel Pinion Gear

Figure 4.45 Normal Stress Distribution for System 4

Table 4.8 Comparison Table for Normal Stress

Results	<i>System 1</i>	<i>System 2</i>	<i>System 3</i>	<i>System 4</i>
Orientation	X Axis	X Axis	X Axis	X Axis
Minimum (MPa)	-5,9009E+02	-1,0458E+03	-1,2423E+03	-6,8492E+02
Maximum (MPa)	465.64	656.69	2056.1	531.23
Minimum Occurs On	Bevel01-1	Bevel02-1	Bevel01-1	Bevel02-1
Maximum Occurs On	Bevel01-1	Bevel01-1	Bevel02-1	Bevel02-1

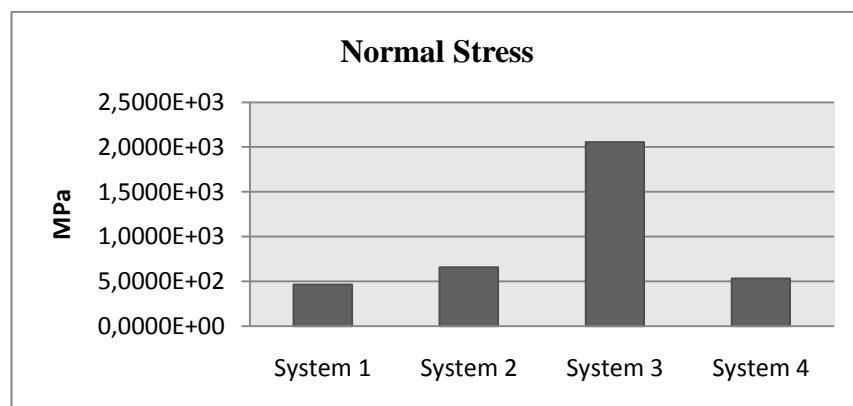


Figure 4.46 Variation of Normal Stress



Figure 4.47 Fractures in the gears.

4.3.3 Deformation Comparison

According to the deformation results, the biggest displacement occurs at the spiral bevel pinion gears teeth that are not in contact. Since the teeth in contact cannot move much, there is less deformation. Table 4.9 shows the total displacement of the gear systems.

4.3.3.1 Total Deformation

Figures 4.48-4.51 show the total deformation distributions in the gears systems. As seen from the figures, the maximum displacements occur at the free teeth as expected.

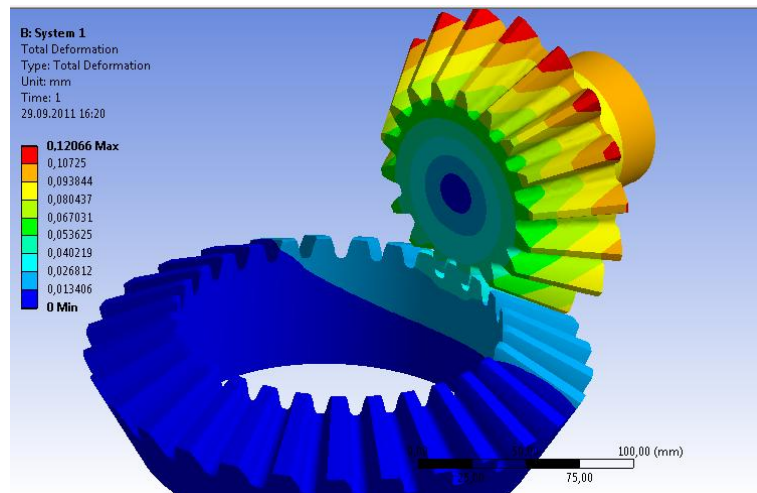


Figure 4.48 Total Deformation for System 1

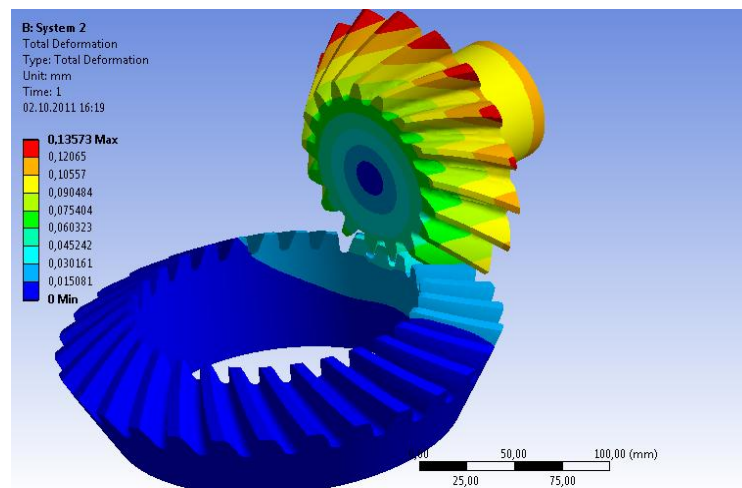


Figure 4.49 Total Deformation for System 2

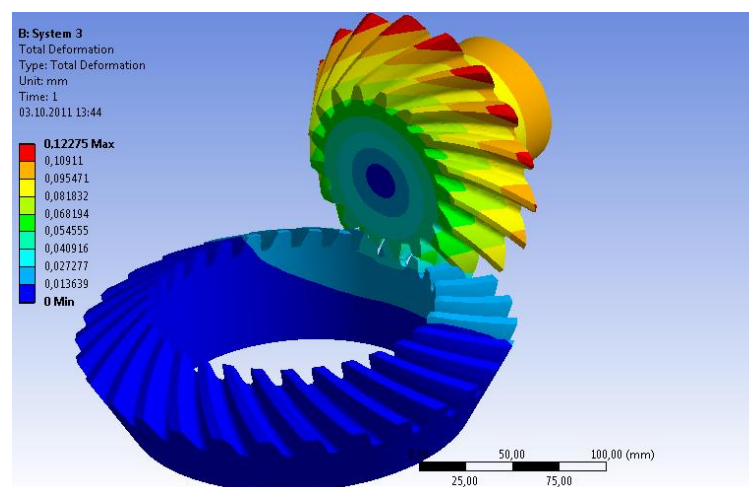


Figure 4.50 Total Deformation for System 3

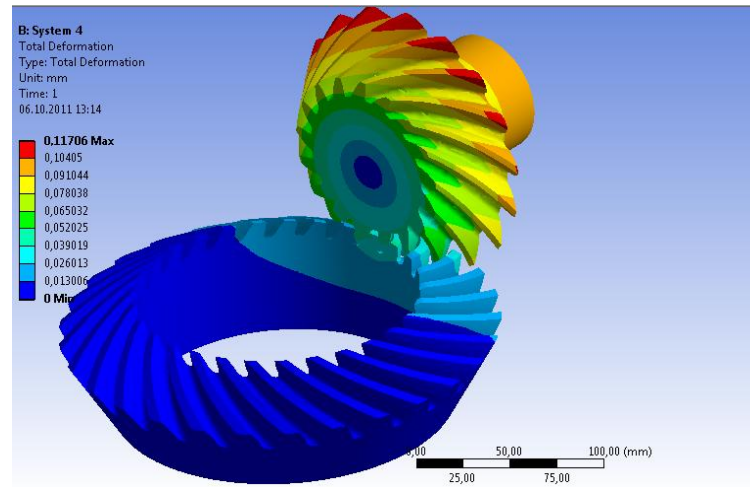


Figure 4.51 Total Deformation for System 4

Table 4.9 Comparison Table for Total Deformation

Results	<i>System 1</i>	<i>System 2</i>	<i>System 3</i>	<i>System 4</i>
Minimum (mm)	0	0	0	0
Maximum (mm)	0.12066	0.13573	0.12275	0.11706
Minimum Occurs On	Bevel01-1	Bevel01-1	Bevel01-1	Bevel01-1
Maximum Occurs On	Bevel02-1	Bevel02-1	Bevel02-1	Bevel02-1

Figure 4.52 shows the variation of the total deformations for the gear systems. As shown in the graphs, the maximum deformation occurs in the System 2.

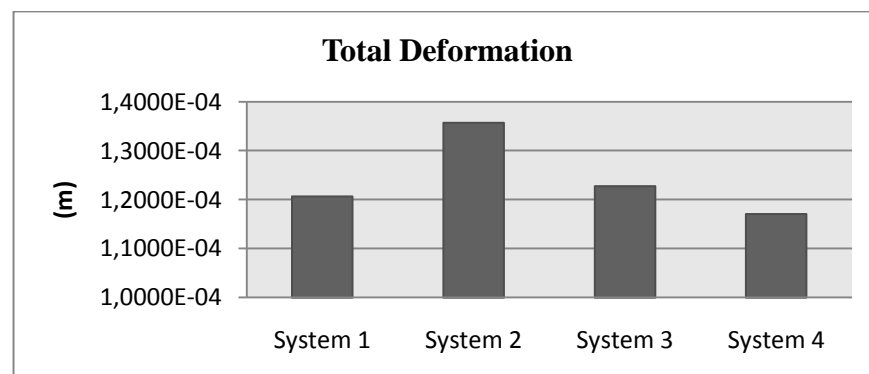


Figure 4.52 Variation of Total Deformation

4.3.3.2 Directional Deformation

Figures 4.53-4.56 show the directional deformation distributions in the gears systems. In this section, the effect of the spiral angles on directional deformation in the x-axis distributions on the gears has been investigated. Figure 4.57 shows the variation of the directional deformations for the gear systems. As shown in the graphs, the maximum deformation occurs in the System 3.

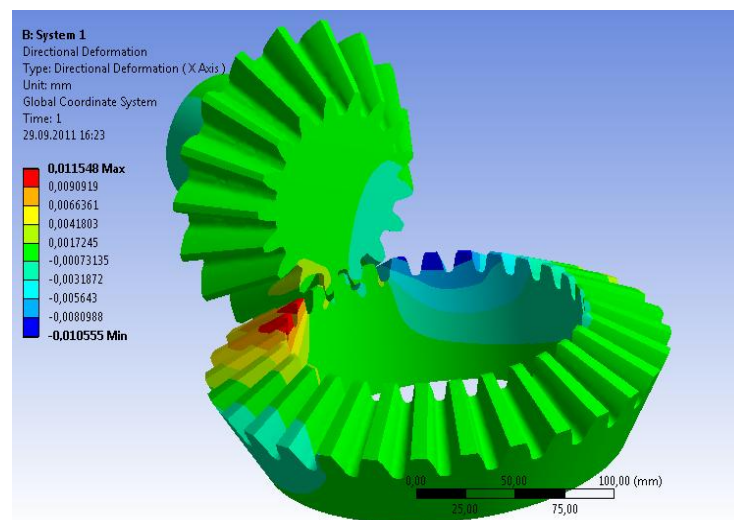


Figure 4.53 Directional Deformation for System 1

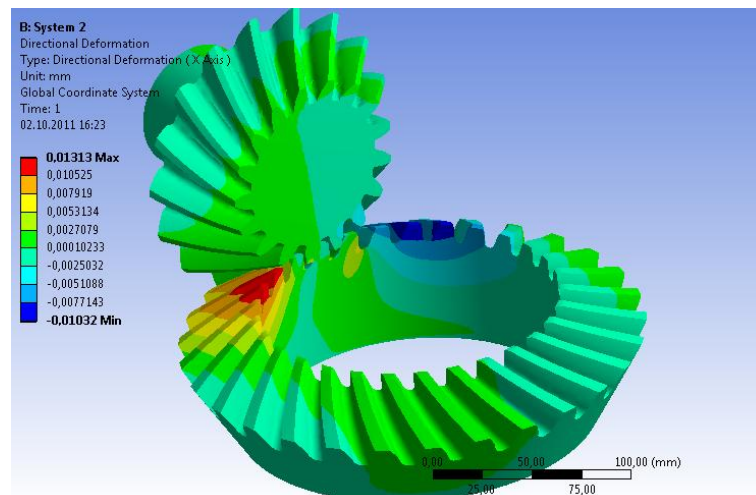


Figure 4.54 Directional Deformation for System 2

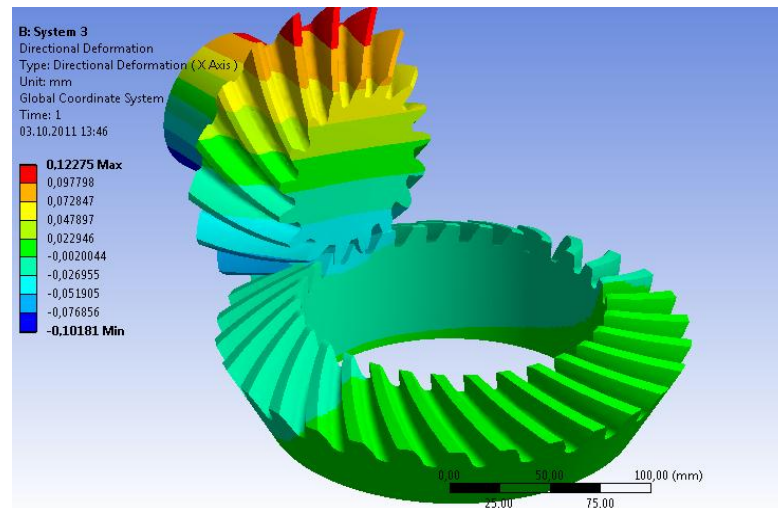


Figure 4.55 Directional Deformation for System 3

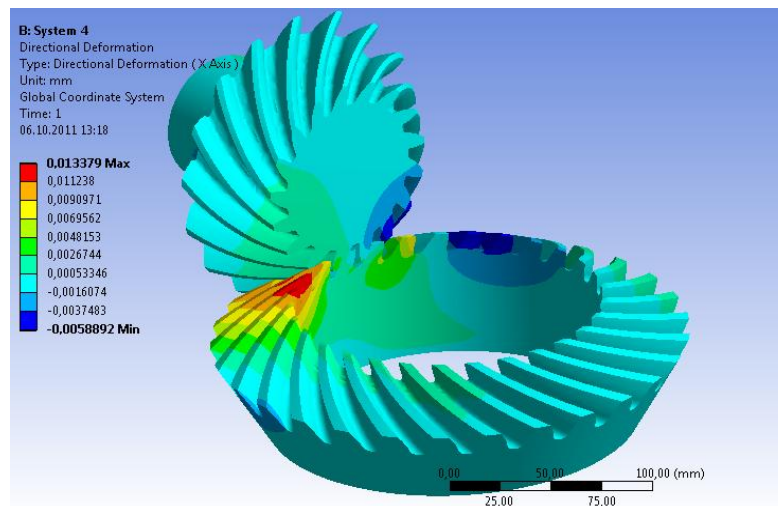


Figure 4.56 Directional Deformation for System 4

Table 4.10 Comparison Table for Directional Deformation

Directional Deformation	<i>System 1</i>	<i>System 2</i>	<i>System 3</i>	<i>System 4</i>
Orientation	X Axis	X Axis	X Axis	X Axis
Minimum (mm)	-1,0555E-02	-1,0320E-02	-1,0181E-01	-5,8892E-03
Maximum (mm)	1,1548E-02	1,3130E-02	1,2275E-01	1,3379E-02
Minimum Occurs On	Bevel01-1	Bevel01-1	Bevel02-1	Bevel02-1
Maximum Occurs On	Bevel01-1	Bevel01-1	Bevel02-1	Bevel01-1

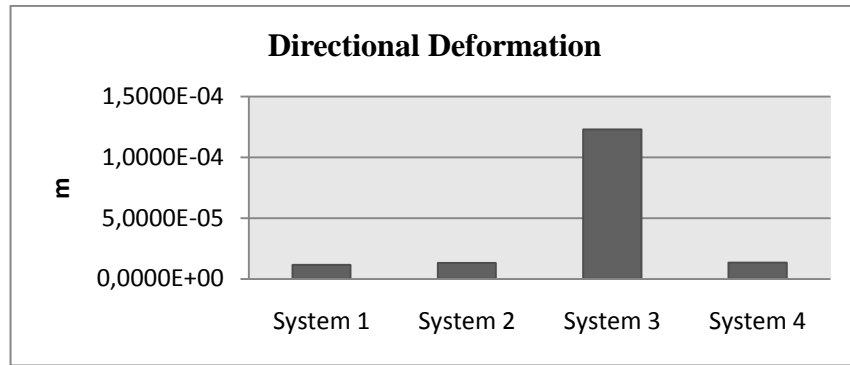


Figure 4.57 Variation of Directional Deformation

4.3.4 Contact Surface Status

Figures 4.58-4.61 show the contact surface status for all gear systems.

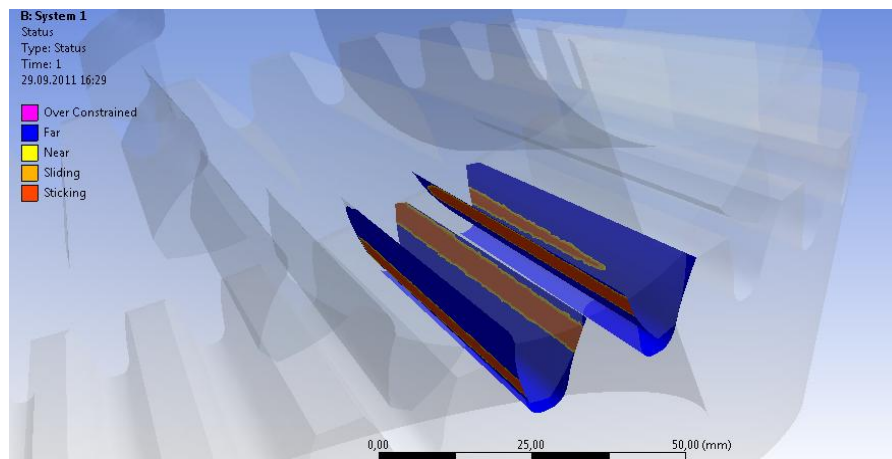


Figure 4.58 Contact Status for System 1

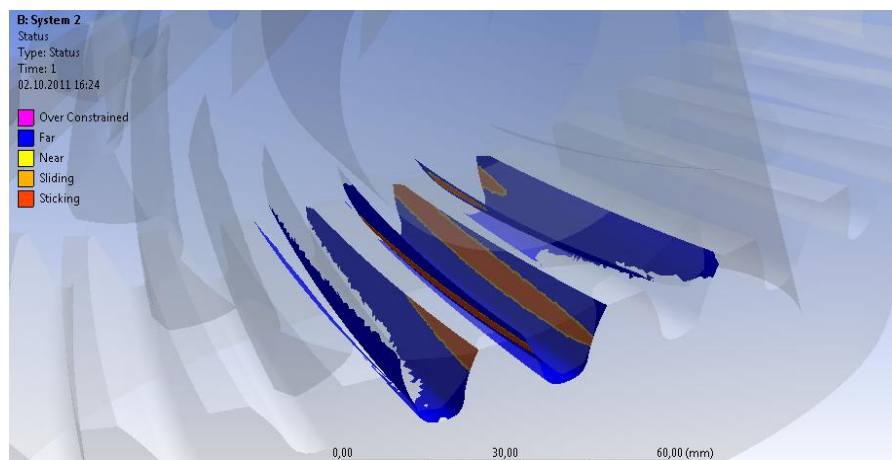


Figure 4.59 Contact Status for System 2

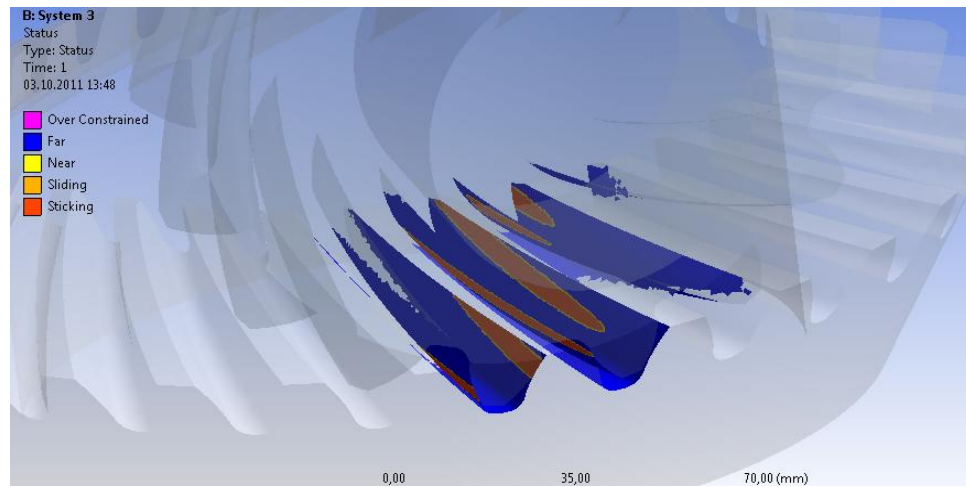


Figure 4.60 Contact Status for System 3

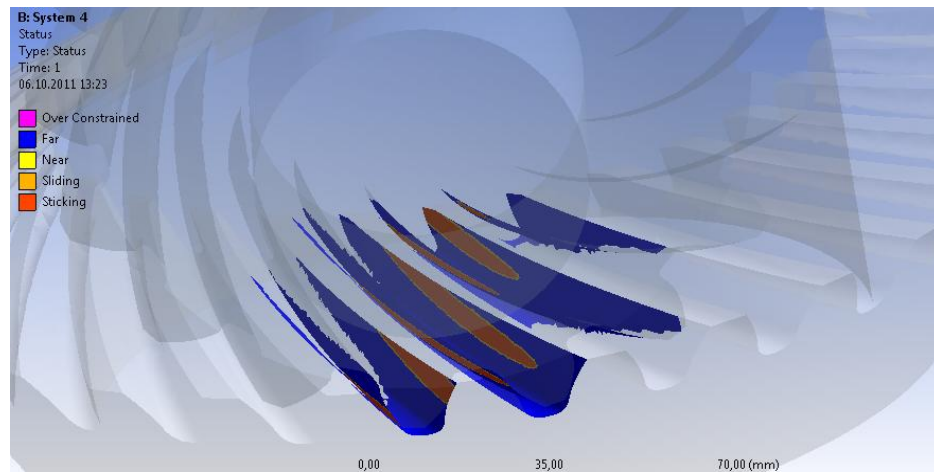
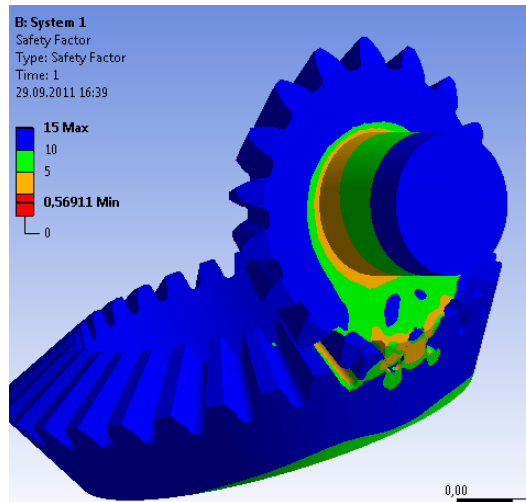


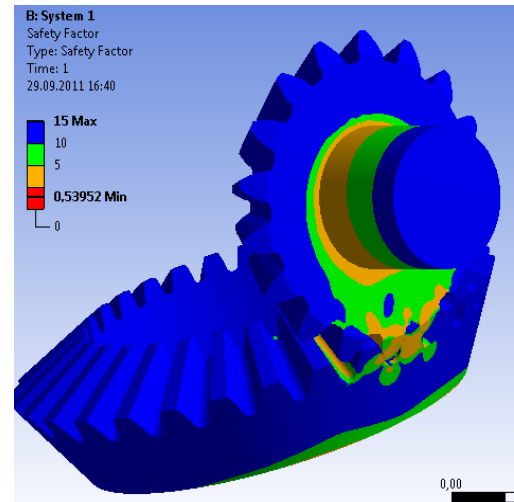
Figure 4.61 Contact Status for System 4

4.3.5 Safety Factor

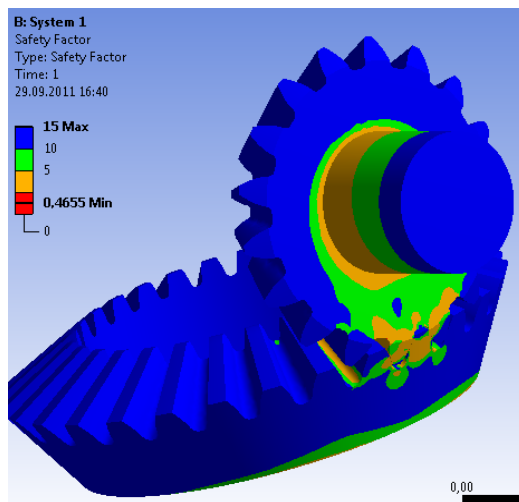
Figures 4.62-65 present the safety factor according to the maximum equivalent stress (part a), maximum shear stress (part b), Mohr-Coulomb stress (part c) and maximum tensile stress (part d) for all gear systems. As known, maximum equivalent stress or von-Mises stress criterion as more common called and maximum shear stress criterion are used for ductile materials. Mohr-Coulomb stress and maximum tensile stress criteria are used for the materials which have brittle material characteristics.



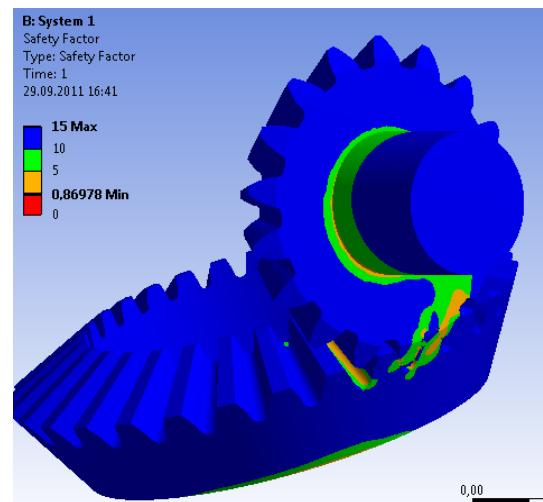
a. Maximum Equivalent Stress



b. Max Shear Stress

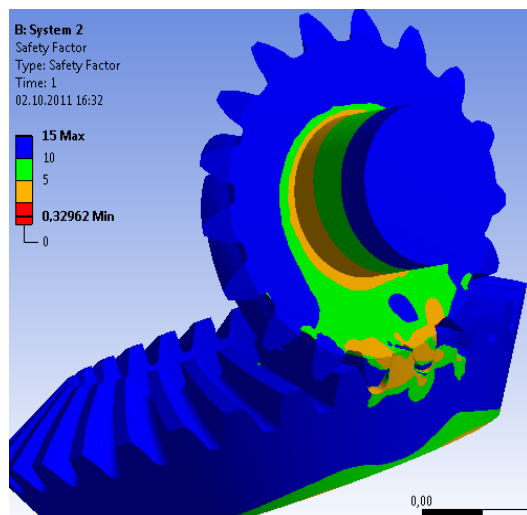


c. Mohr-Coulomb Stress

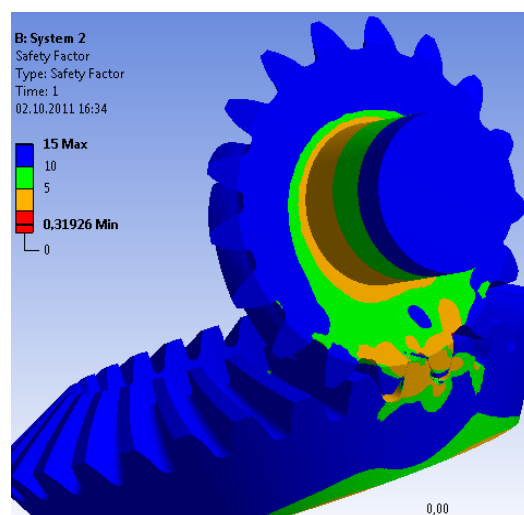


d. Maximum Tensile Stress

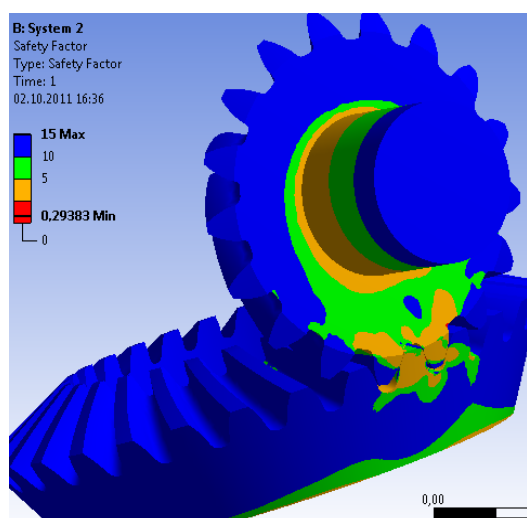
Figure 4.62 Safety Factors for System 1



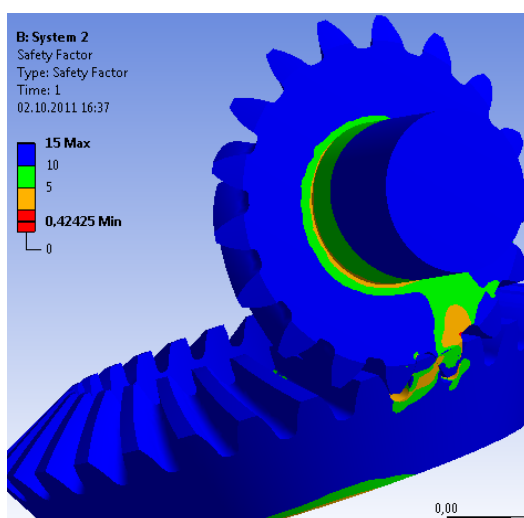
a. Maximum Equivalent Stress



b. Maximum Shear Stress

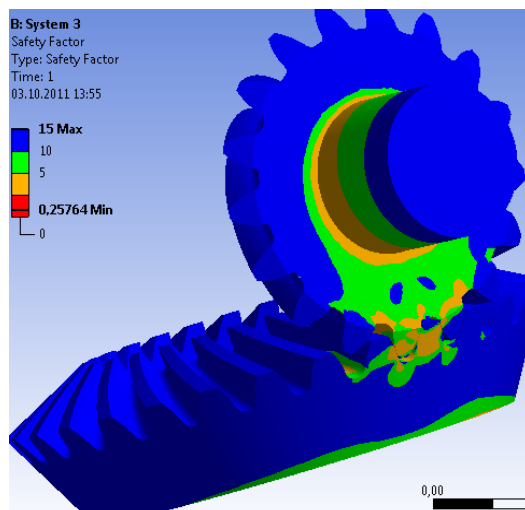


c. Mohr-Coulomb Stress

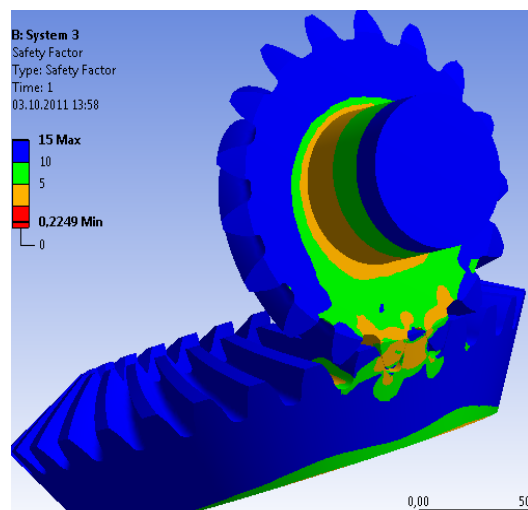


d. Maximum Tensile Stress

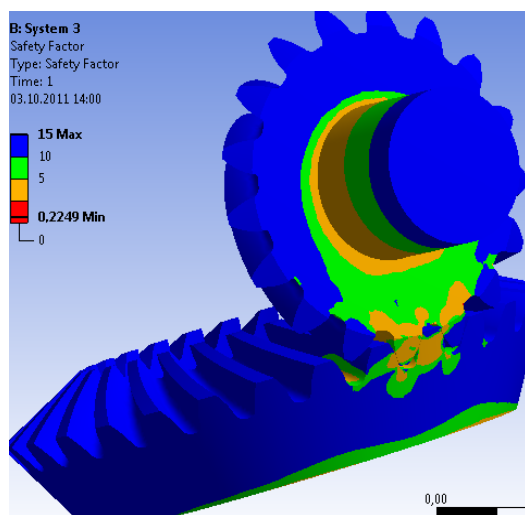
Figure 4.63 Safety Factors for System 2



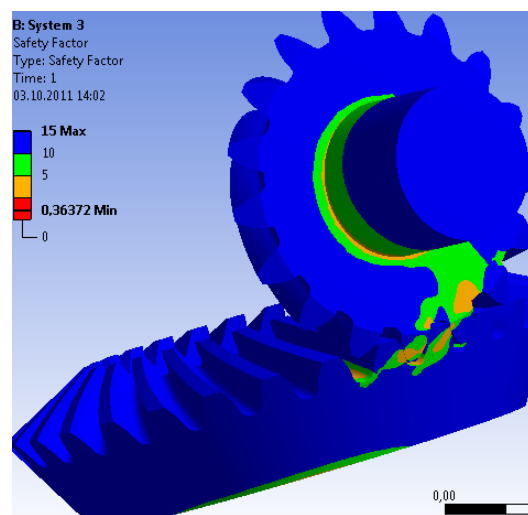
a. Maximum Equivalent Stress



b. Maximum Shear Stress



c. Mohr-Coulomb Stress



d. Maximum Tensile Stress

Figure 4.64 Safety Factors for System 3

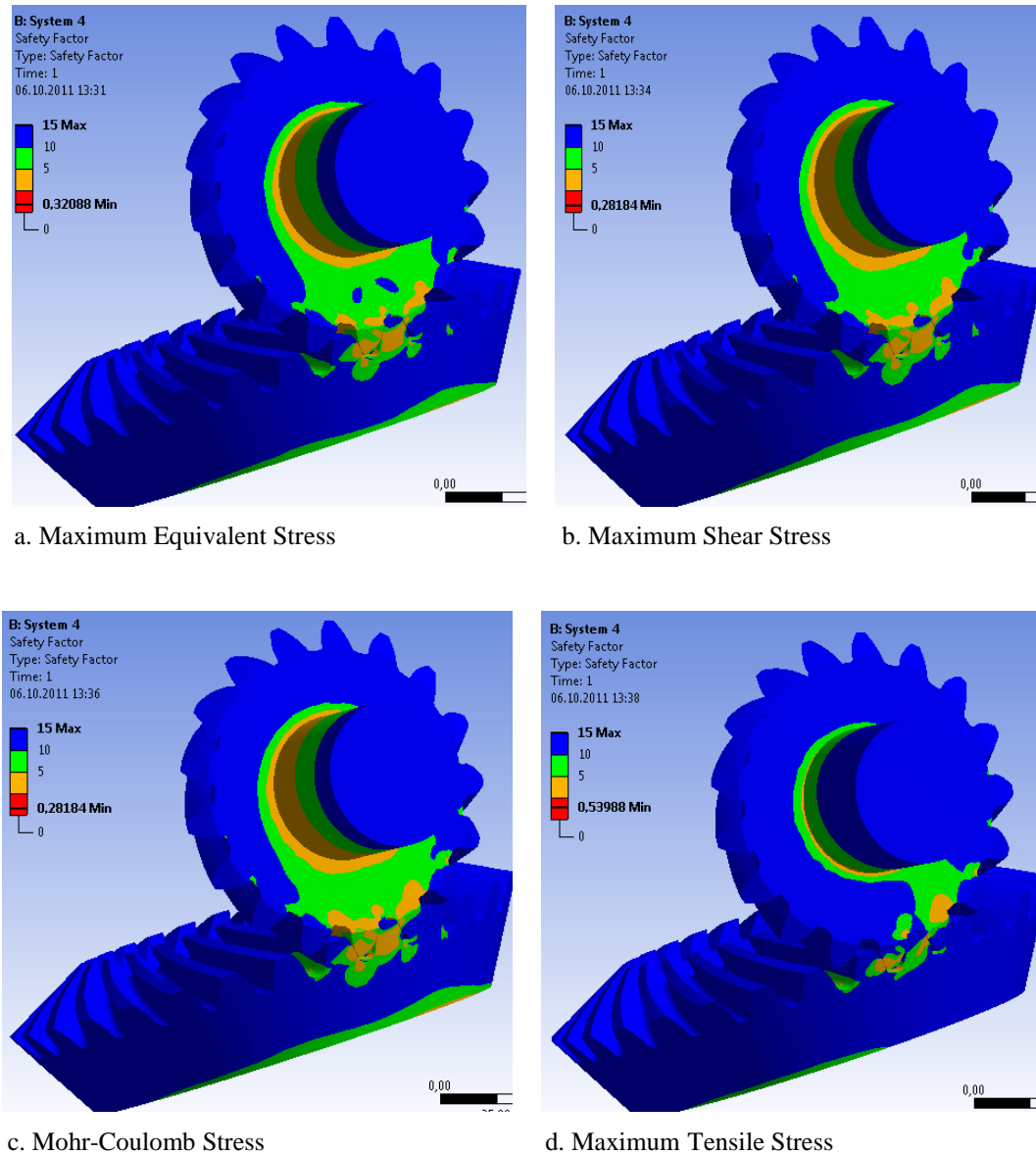


Figure 4.65 Safety Factors for System 4

Tables 4.11-4.14 presents the maximum equivalent stress, maximum shear stress, Mohr-Coulomb stress and maximum normal stress safety factor values, respectively.

Table 4.11 Comparison Table of Max Equivalent Stress Safety Factor

<i>Max Equivalent Stress</i>				
<i>Safety Factor</i>	System 1	System 2	System 3	System 4
Minimum	0,56911	0,32962	0,25764	0,32088
Minimum Occurs On	Bevel01-1	Bevel01-1	Bevel02-1	Bevel02-1

Table 4.12 Comparison Table of Maximum Shear Stress Safety Factor

<i>Max Shear Stress Safety Factor</i>	System 1	System 2	System 3	System 4
Minimum	0,53952	0,31926	0,2249	0,28184
Minimum Occurs On	Bevel01-1	Bevel01-1	Bevel02-1	Bevel02-1

Table 4.13 Comparison Table of Mohr-Coulomb Stress Safety Factor

<i>Mohr-Coulomb Stress Safety Factor</i>	<i>System 1</i>	<i>System 2</i>	<i>System 3</i>	<i>System 4</i>
Minimum	0,4655	0,29383	0,2249	0,28184
Minimum Occurs On	Bevel01-1	Bevel01-1	Bevel02-1	Bevel02-1

Table 4.14 Comparison Table of Maximum Tensile Stress Safety Factor

<i>Max Tensile Stress Safety Factor</i>	<i>System 1</i>	<i>System 2</i>	<i>System 3</i>	<i>System 4</i>
Minimum	0,86978	0,42425	0,36372	0,53988
Minimum Occurs On	Bevel01-1	Bevel01-1	Bevel02-1	Bevel01-1

Figures 4.66-4.69 illustrate the variation of the safety factors with respect to the type of gear systems. As shown in the graphs, the maximum safety factor has been obtained using the System 1.

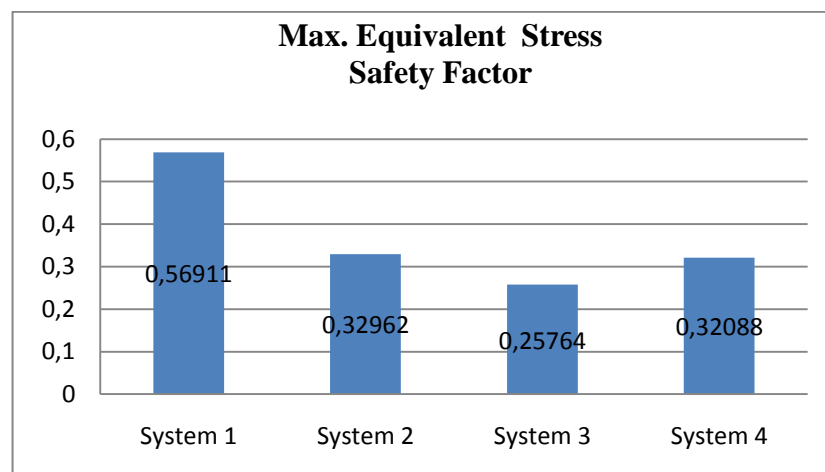


Figure 4.66 Variation of Maximum Equivalent Stress Safety Factor

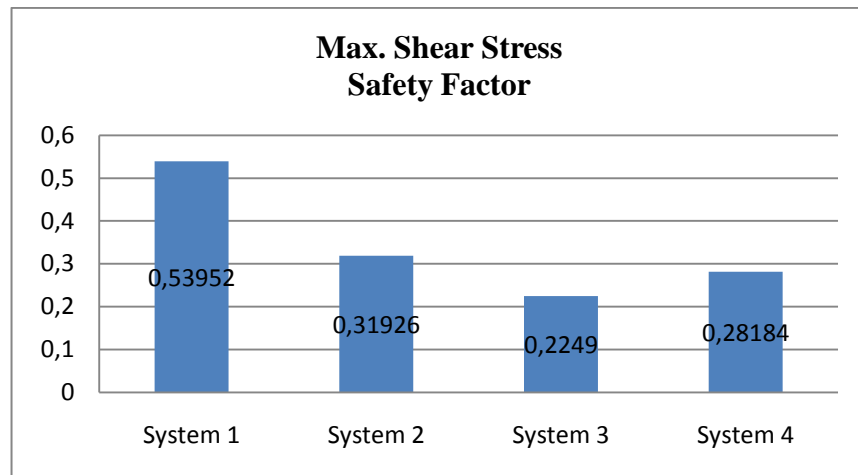


Figure 4.67 Variation of Maximum Shear Stress Safety Factor

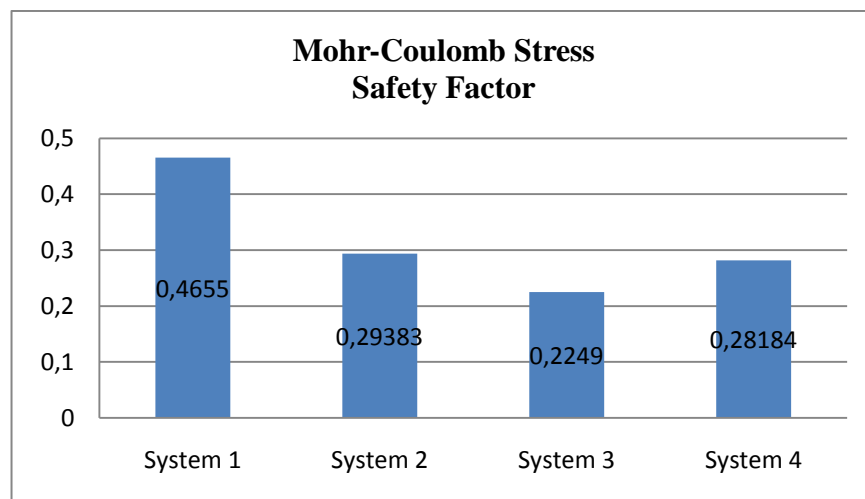


Figure 4.68 Variation of Mohr-Coulomb Stress Safety Factor

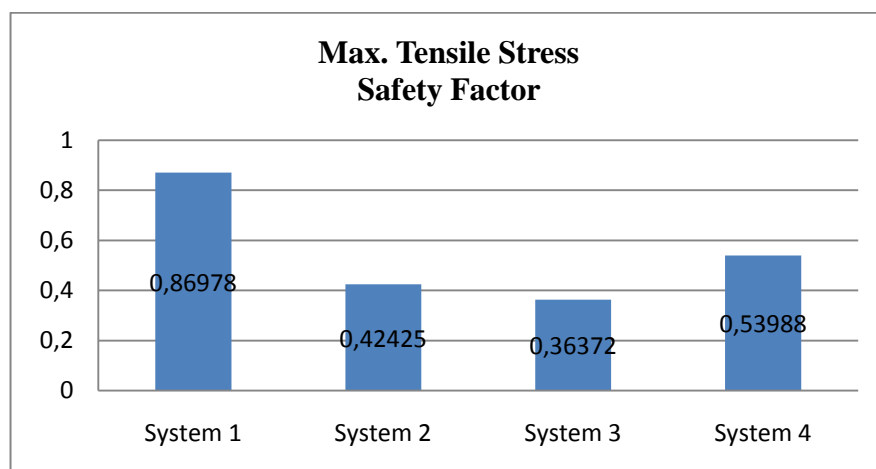


Figure 4.69 Variation of Maximum Tensile Stress Safety Factor

CHAPTER FIVE

CONCLUSIONS

In this study, the effect of the spiral bevel gear spiral angles on the stress, strain and deformation on the gear systems have investigated in order to determine the most proper gear system for the differential. In order to avoid the unexpected fractures of the gear teeth, four different gear groups have been selected; computer-aided modeling and the finite element contact analyses have been performed. The conclusions are summarized as follows:

1. For spiral angles higher than 34° , the teeth dimensions and compression areas increase, causing to decrease the strain and stress values due to escalating curvature of spiral bevel gears' teeth.
2. Considering the analyses, the lowest stress values have been observed at 43° and 25° spiral angles. It should be noted that the gear groups examined in this study had a maximum of 43° angle. Other studies have shown that really high spiral angle values resulted in rapidly increasing stress levels.
3. When the correlation between helix angles and stress values is examined, it is seen that as the helix angle increases so does the stress value increases. Addendum stress increase until helix angle is $17,70^{\circ}$, dedendum stress increase until helix angle is $21,39^{\circ}$ and for higher angles, both stress values start decreasing. Disregarding very small helix angle values, the minimum addendum stress is observed when the helix angle is $35,24^{\circ}$ and the minimum dedendum stress is obtained when the helix angle is $43,98^{\circ}$. For respectively higher values of helix angle, the stress levels increase rapidly. Because, the gear teeth get extremely close to each other and teeth interferences increase for the helix angle values higher than 45° due to geometrical limitations. Hence, higher helix values than 45° are not preferred for bevel gearwheels (Erdin, 2009).

4. The gears in the systems examined which have brittle characteristics due to the heat treatment processes. Hence, the normal stress results show that, the most logical choice is the 43^0 spiral angled gear group for spiral bevel gears.

REFERENCES

- Akkurt, M. (2000). *Makina elemanları Cilt I-II*. İstanbul: Birsen Yayınevi.
- Argyris, J., Fuentes, A., & Litvin F. L. (2002). Computerized integrated approach for design and stress analysis of spiral bevel gears. *Computer Methods in Applied Mechanics and Engineering*, 191, 1057-1095.
- Aymaksan Dişli (n.d.). *Spiral Konik Dişliler: Özet Bilgi, Kullanım Alanları ve Uygulama Resimleri*. Retrieved February 02, 2011, from http://www.aymaksan.biz/tr/urunlerimiz_spiral_konik_disli_ayna_mahruti_disli.html
- Bathe, K. J. (2008). The finite element method. B. W. Wah, (Ed.), *Wiley Encyclopedia of Computer Science and Engineering* (1-12). John Wiley & Sons, Inc.
- Bevel gears. (n.d.) Retrieved April 2, 2011, from http://www.roymech.co.uk/Useful_Tables/Drive/Bevel_Gears.html
- Bloch, H. P., & Geitner, F. K. (1996). Major process equipment maintenance and repair. *Practical machinery management for process plants*, 4 (2 nd ed.). Houston, Texas: Gulf Publishing Company.
- BÖHLER-UDDEHOLM Australia (n.d.). *EN36A case hardening steel*. Retrieved August 31, 2011, from http://www.buau.com.au/english/files/MW_EN36A.pdf
- Brown, M. D. (2009). *Design and analysis of a spiral bevel gear*. Master of Engineering in Mechanical Engineering. Hartford, Connecticut: Rensselaer Polytechnic Institute.

Daimler-Benz AG (n.d.). *Technical Data Mercedes-Benz Industrial Diesel Engine, OM 447*

Doğanay, T. (1963). *Dişli çarklar*. İstanbul: Arı Kitabevi Matbaası

Erdin, M. E. (2009). *Helisel konik dişli çarklarda gerilmelerin sonlu eleman yöntemiyle incelenmesi*. Ph. D. Thesis. Ankara: Institute of Science and Technology of Gazi University.

Huebner, K. H., Dewhurst, D. L., Smith, D. E., & Byrom, T. G. (2001). *The finite element method for engineers*. Canada: John Wiley&Sons, Inc.

Lin, T., Ou, H., & Li, R. (2007). A finite element method for 3D static and dynamic contact/impact analysis of gear drives. *Computer Methods in Applied Mechanics and Engineerin*, 196, 1716-1728.

Litvin, F. L., Fuentes, A., & Hayasaka, K. (2006). Design, manufacture, stress analysis, and experimental tests of low-noise high endurance spiral bevel gears. *Mechanism and Machine Theory*, 41, 83–118.

Litvin, F. L., Fuentes, A., Fan, Q., & Handschuh, R. F. (2002). Computerized design, simulation of meshing, and contact and stress analysis of face-milled formate generated spiral bevel gears. *Mechanism and Machine Theory*, 37, 441-459.

Litvin, F. L., Wang, A. G., & Handschuh, R. F. (1998). Computerized generation and simulation of meshing and contact of spiral bevel gears with improved geometry. *Computer Methods in Applied Mechanics and Engineerin*, 158, 35-64.

Oberg, E., Jones, F. D., Horton, H. L., & Ryffel, H. H. (2008) *Machinery's Handbook* (28th ed.). New York: Industrial Press.

- Roylance, D. (2001). *Finite element analysis*. Cambridge: Department of Materials Science and Engineering, Massachusetts Institute of Technology.
- Sheveleva, G. I., Volkov, A. E., & Medvedev V. I. (2007). Algorithms for analysis of meshing and contact of spiral bevel gears. *Mechanism and Machine Theory*, 42, 198-215.
- Shigley, J. E., Mischke, C. R., & Budynas, R. G. (2004). *Mechanical engineering design* (7th ed.). New York: The McGraw Hill Companies.
- Simon, V. (2000). FEM stress analysis in hypoid gears. *Mechanism and Machine Theory*, 35, 1197-1220.
- Simon, V. (2007). Computer simulation of tooth contact analysis of mismatched spiral bevel gears. *Mechanism and Machine Theory*, 42, 365-381.
- Taylor, R. L. (2011). *A finite element analysis program*. California: Department of Civil and Environmental Engineering University of California at Berkeley.
- Tsai, Y. C., & Hsu, W. Y. (2008). The study on the design of spiral bevel gear sets with circular-arc contact paths and tooth profiles. *Mechanism and Machine Theory*, 43, 1158-1174.
- Whitmire, G. (2003). *Drafting manual*. Amsterdam: Genium Publishing Corporation